

Test Report

Report No.: ZIR-200211-rev0

Date: 20-March-2020

Test specimen:

Ceramic Dental Implants

Test method:

Finite Element Analysis

Customer:

**ZIRKONUS Implantatsysteme
Dr. Dr. Gerd A. Walther
Heerweg 15 D
73770 Denkendorf
GERMANY**

Examiner:

**Dr. Stur & Pfeufer Beratende Ingenieure PartGmbB
Dr.-Ing. Stephan Stur
Wagmüllerstr. 16
80538 München
GERMANY**

Signature: _____



Dr.-Ing. Stephan Stur



Dipl.-Ing. Paul Pfeufer

Notice:

The test results relate only to the items tested!

Index

| | | |
|-------|--|----|
| 1 | Subcontractors | 3 |
| 2 | Specimens..... | 3 |
| 3 | Objective | 4 |
| 4 | Test Procedure | 11 |
| 4.1 | Model description | 11 |
| 4.1.1 | Test setups | 11 |
| 4.2 | Test Equipment | 14 |
| 4.3 | Test Description..... | 14 |
| 4.3.1 | Material properties | 14 |
| 4.3.2 | FE models..... | 15 |
| 5 | Results | 26 |
| 5.1 | FEA model 1 (CAD model IM-R11_standard) | 26 |
| 5.2 | FEA model 2 (CAD model IM-R11_individuell) | 30 |
| 5.3 | FEA model 3 (CAD model IE-SST-L11) | 32 |
| 5.4 | FEA model 4 (CAD model IE-SBE-L11)..... | 34 |
| 5.5 | FEA model 5 (CAD model IE-SST-L11) | 36 |
| 5.6 | FEA model 6 (CAD model IE-R-L11) | 38 |
| 5.7 | FEA model 7 (CAD model IM-R11_standard) | 40 |
| 5.8 | FEA model 8 (CAD model IM-R11_standard) | 42 |
| 5.9 | FEA model 9 (CAD model IM-2x_R11_indi-Abut_Bridge_11G)..... | 44 |
| 5.10 | FEA model 10 (CAD model IM-2x_R11_stand-Abut_angeh-Bridge) | 46 |
| 5.11 | FEA model 11 (CAD model ZSystems Z5c)..... | 52 |
| 6 | Conclusion..... | 56 |

1 Subcontractors

None

2 Specimens

Ceramic Dental Implants. CAD models:

CAD model 1 (IM-R11_standard):

Original CAD file name 'bg_im-r-stand_pruefv_asm.stp', received 05-Feb-2020

CAD model 1b (IM-R11_standard with gap):

Original CAD file name 'bg_impl_im-r-stand_m-spalt.stp', received 16-Mar-2020

Note: CAD model 1b is based on CAD model 1 with a cement layer between implant shoulder and loading member

CAD model 2 (IM-R11_individuell):

Original CAD file name 'bg_impl_im-r_11G.stp', received 26-Feb-2020

CAD model 3 (IE-SST-L11):

Original CAD file name 'bg_ie-sst_pruefkuppe_asm.stp', received 05-Feb-2020

CAD model 4 (IE-SBE-L11):

Original CAD file name 'bg_ie-sbe_pruefvorrichtung_asm.stp', received 05-Feb-2020

CAD model 5 (IE-R-L11):

Original CAD file name 'bg_ie-r_pruefvorrichtung_asm.stp', received 05-Feb-2020

CAD model 6 (IM-2x_R11_indi-Abut_Bridge_11G):

Original CAD file name 'bg_im-r_pk-bridge_asm.stp', received 05-Feb-2020

CAD model 7 (IM-2x_R11_stand-Abut_angeh-Bridge):

Original CAD file name 'bg_im-r_ang-bridge_asm.stp', received 26-Feb-2020

CAD model 8 (ZSystems Z5c):

Original CAD file name 'bg_z5c_asm.stp', received 21-Feb-2020

Material data for the Zirkonus models 1-7:

Taken from test report WAL-080504_rev0 from 21-Jul-2008

Material data for the ZSystems model 8:

Taken from file 'PANAVIA-Technische-Daten-2020-02-21.docx' received 21-Feb-2020

3 Objective

The objective of the examination is the determination of the static stress values in different dental implant systems with no pre-angled and pre-angled connecting parts using Finite Element Analysis. Set-up and loading conditions of the dental implant system were realized according to ISO 14801 (2016) and according to setups provided by the customer.

Fig. 1 to Fig. 11 show the CAD models of the implant systems examined (cross-section).

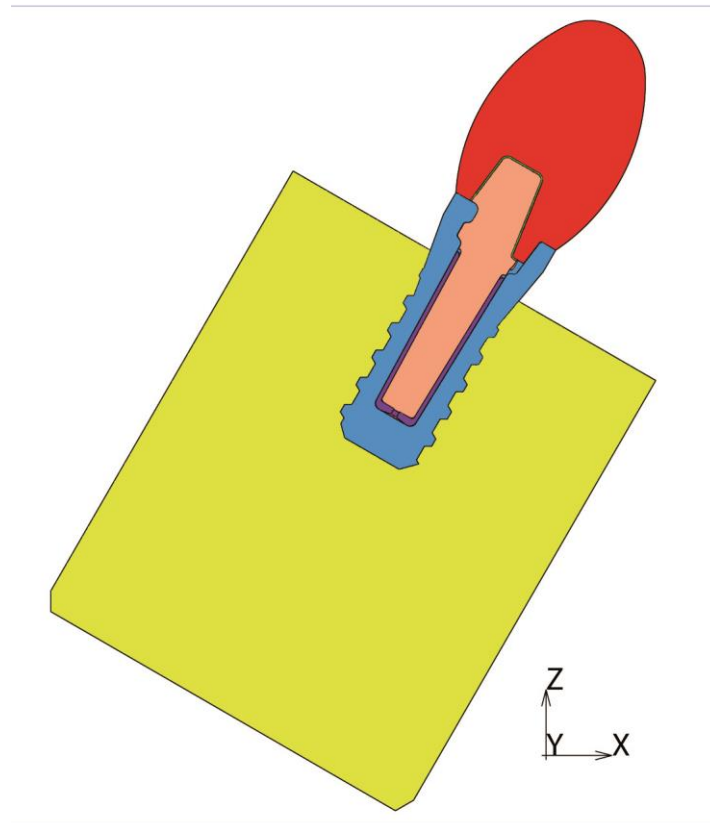


Fig. 1: CAD model of implant system model 1 (IM-R11_standard; + 30°).

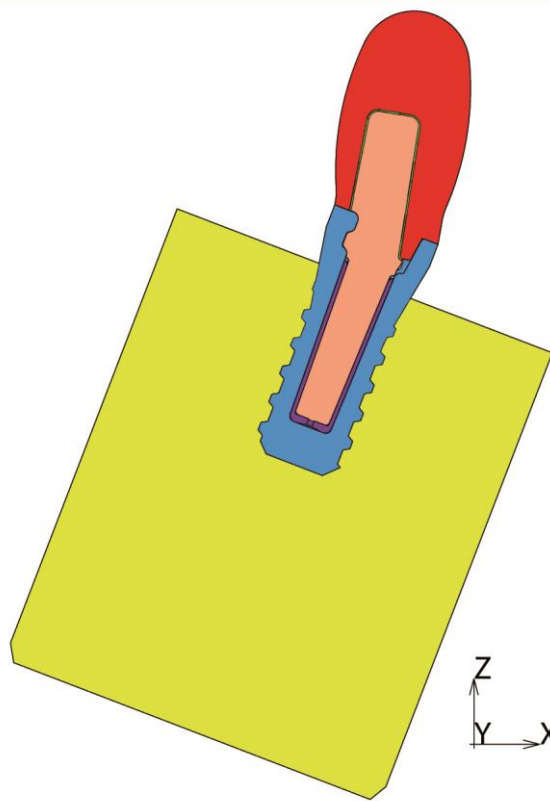


Fig. 4: CAD model of implant system model 2 (IM-R11_individuell; +21°).

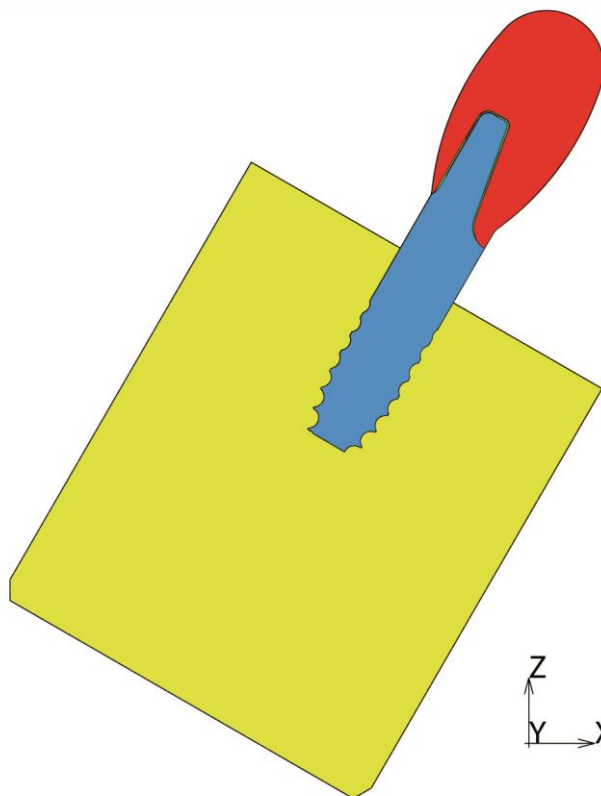


Fig. 5: CAD model of implant system model 3 (IE-SST-L11; +30°).

Date: 20-Mar-2020 Signature: _____ *sk*

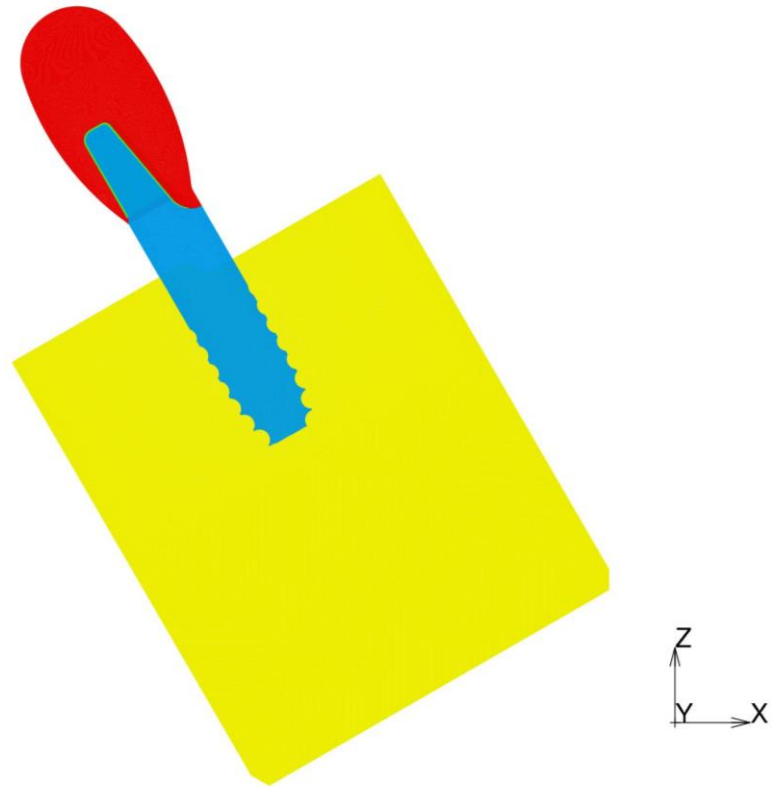


Fig. 6: CAD model of implant system model 3 (IE-SST-L11; -30°).

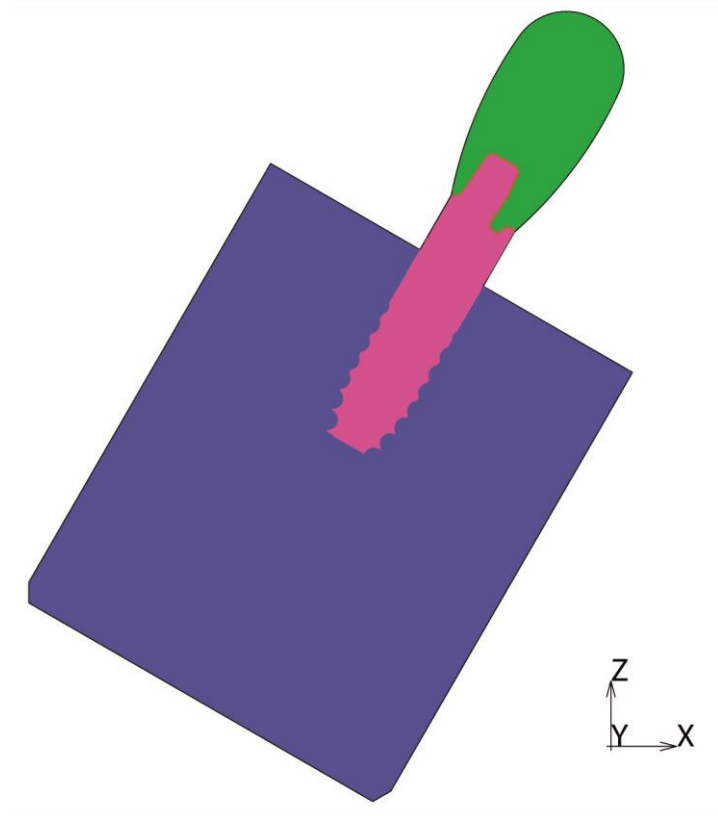


Fig. 7: CAD model of implant system model 4 (IE-SBE-L11; +30°).

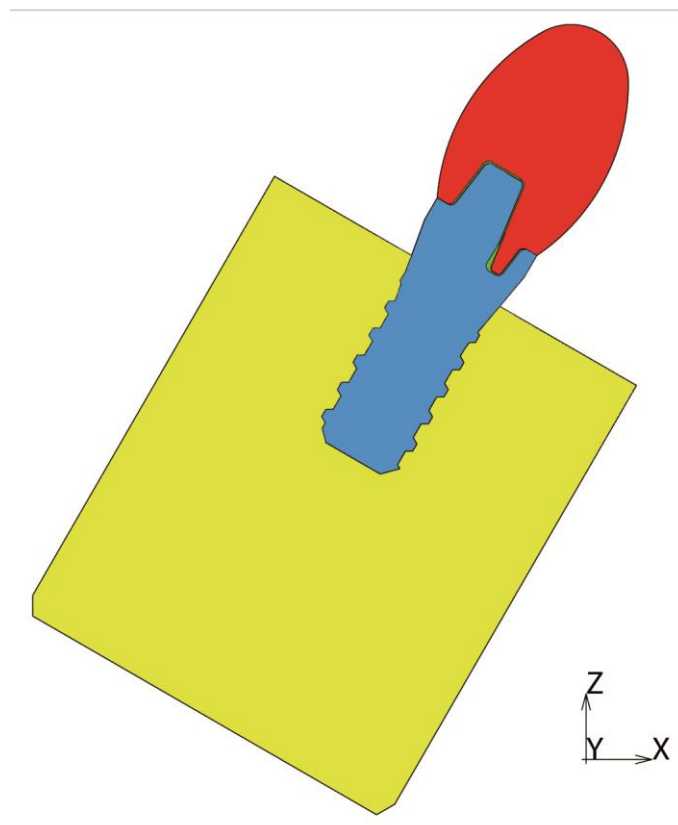


Fig. 8: CAD model of implant system model 5 (IE-R-L11; + 30°).

4 Test Procedure

4.1 Model description

4.1.1 Test setups

Finite Element Analysis (FEA) has been used to examine different dental implant systems. Three-dimensional FE models were used to simulate the setup and loading conditions according to ISO 14801 (2016). Fig. 12 and Fig. 13 show the general set-ups for the loading of implant systems with both non-angulated and angulated abutments.

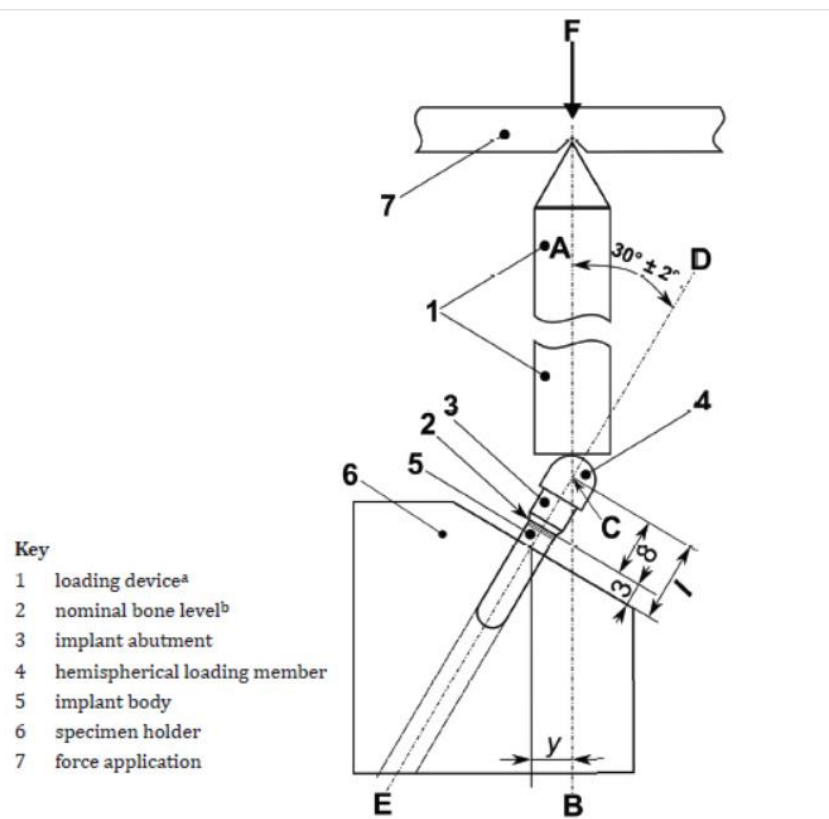


Fig. 12: Test setup for non-angulated abutments according to ISO 14801 (2016).

The FEA model with the angulated abutment (CAD model 2: IM-R11_individuell) has been examined according to Fig. 13 resulting in an overall tilt of the support of 21° ($\alpha = 11^{\circ}$); all other models were loaded with a tilt of 30° according to Fig. 12.

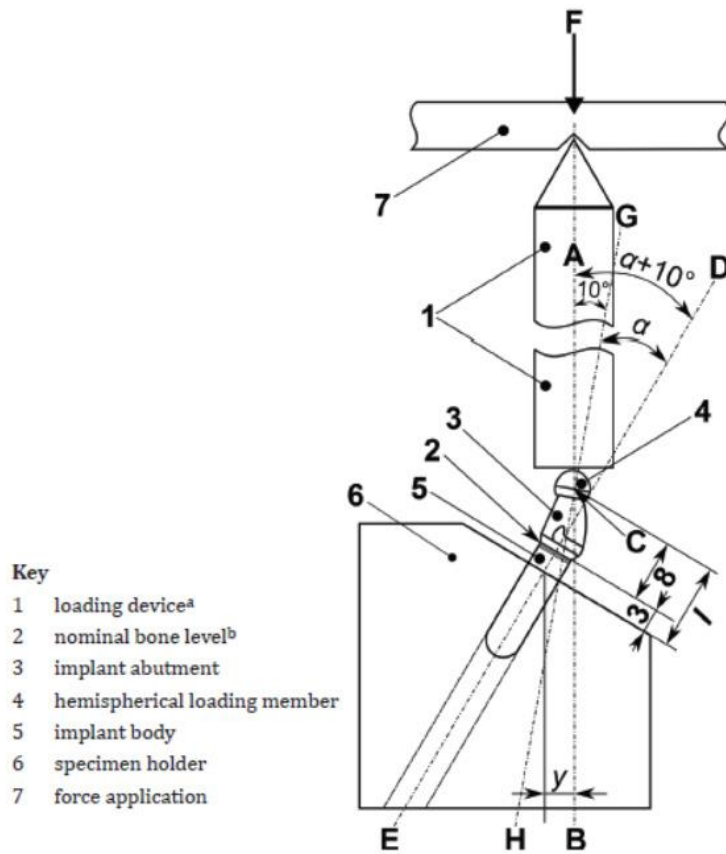


Fig. 13: Test setup for angulated abutments according to ISO 14801 (2016).

The simulation of the screw-in of the abutment into the sleeve/implant body (FEA model 8) was realized using a 120° model of the three components from FEA model 1).

Tab. 1 shows the overview of all CAD and FEA models examined.

Tab. 1: List of all models and analyses performed.

| FEA model | CAD model / assembly | Description and setup |
|-----------|--|---|
| 1 | Model 1 (IM-R11_standard) | 1. Push-in of the abutment into the sleeve/implant body 2. 200 N loading under +30° according to ISO 14801. |
| 1b | Model 1b (IM-R11_standard with gap) | 1. Push-in of the abutment into the sleeve/implant body 2. 200 N loading under +30° according to ISO 14801. |
| 2 | Model 2 (IM-R11_individuell) | 1. Push-in of the abutment into the sleeve/implant body 2. 200 N loading under +21° according to ISO 14801. |
| 3 | Model 3 (IE-SST-L11) | 200 N loading under +30° according to ISO 14801 |
| 4 | Model 4 (IE-SBE-L11) | 200 N loading under +30° according to ISO 14801 |
| 5 | Model 3 (IE-SST-L11) | Variation of the load: 200 N loading under -30° according to ISO 14801. |
| 6 | Model 5 (IE-R-L11): | 200 N loading under +30° according to ISO 14801 |
| 7 | Model 1 (IM-R11_standard) | Variation of the load: 200 N loading under -30° according to ISO 14801 |
| 8 | Model 1 (IM-R11_standard) | Simulation of the screw-in of the abutment into sleeve/implant body |
| 9 | Model 6 (IM-2x_R11_indi- Abut_Bridge_11G) | 1. Push-in of the abutment into the sleeve/implant body 2. 200 N loading of the bridge (clearance 10mm) under +30° according to ISO 14801. |
| 10 | Model 7 (IM-2x_R11_stand- Abut_angeh-Bridge) | 1. Push-in of the abutment into the sleeve/implant body 2. 200 N loading of the bridge (clearance 5mm) under +30° according to ISO 14801. |
| 11 | Model 8 (ZSystems Z5c) | 200 N loading under +30° according to ISO 14801. |

4.2 Test Equipment

The FE simulations were carried out using the FE program MSC.MARC 2019, for pre- and post-processing the program MSC.MENTAT 2019 (both MSC.Software, Newport Beach, CA, USA) was used.

4.3 Test Description

4.3.1 Material properties

Tab. 2 shows the properties of the materials used in the FE simulations.

Tab. 2: Material properties of the components.

| Component | Material | Young's modulus | Poisson ratio |
|-------------------------------------|----------------------|-----------------|---------------|
| Loading member | Zirconia | 210 GPa | 0.33 |
| Implant body | Zirconia | 210 GPa | 0.33 |
| Abutment | Zirconia | 210 GPa | 0.33 |
| Sleeve | POM | 3.0 GPa | 0.45 |
| Embedding | Bone layer | 6.0 GPa | 0.30 |
| Dental cement | Glass Ionomer Cement | 4.0 GPa | 0.42 |
| Dental cement for CAD model 8 (Z5c) | PANAVIA™ V5 | 6.3 GPa | 0.40 |

4.3.2 FE models

The FE meshes consist of three-dimensional tetrahedral elements with isotropic elastic material behavior. In the FE models second order 10-node tetrahedron elements with improved bending characteristics are used.

Fig. 14 to Fig. 32 show the three-dimensional meshes of embedding, implant and loading member for all models.

In all models the cement bonding has been modeled as a fixed ('glued') contact between the cement and the adjacent body. Also between implant body and the embedding a fixed connection ('glued contact') was modeled. In all other contact regions real contact with the possibility of separation was used.

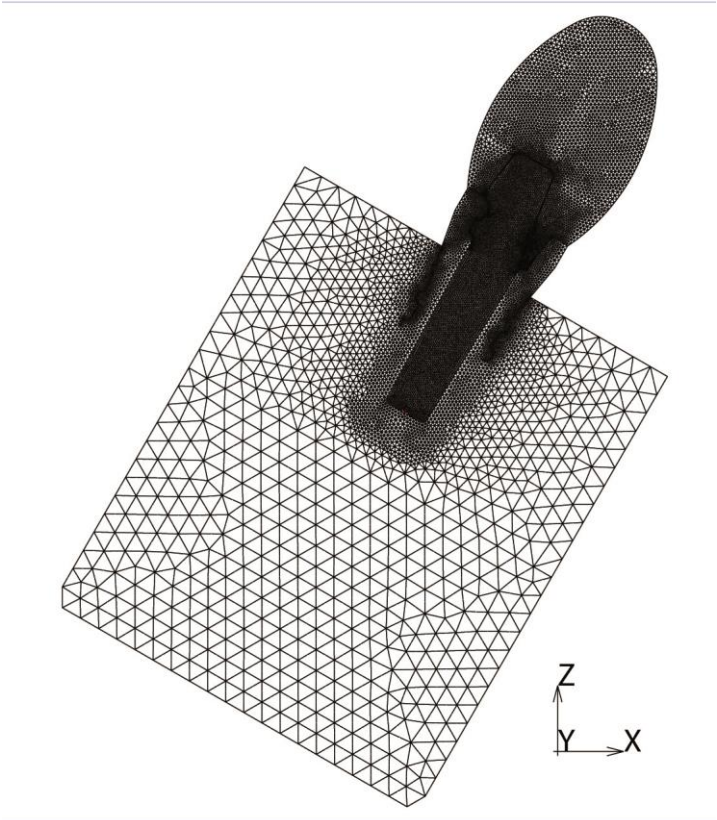


Fig. 14: FE mesh of CAD model 1 (IM-R11_standard; +30°) with 1076818 elements, 1694004 nodes.

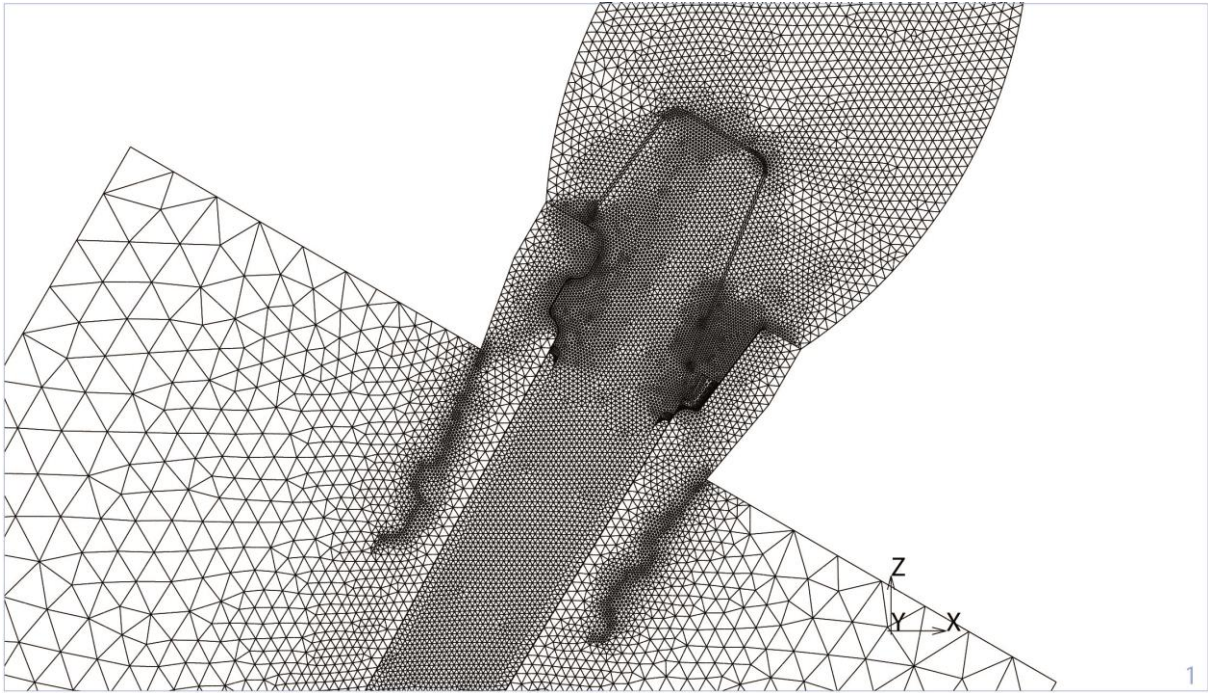


Fig. 15: Detail of Fig. 14.

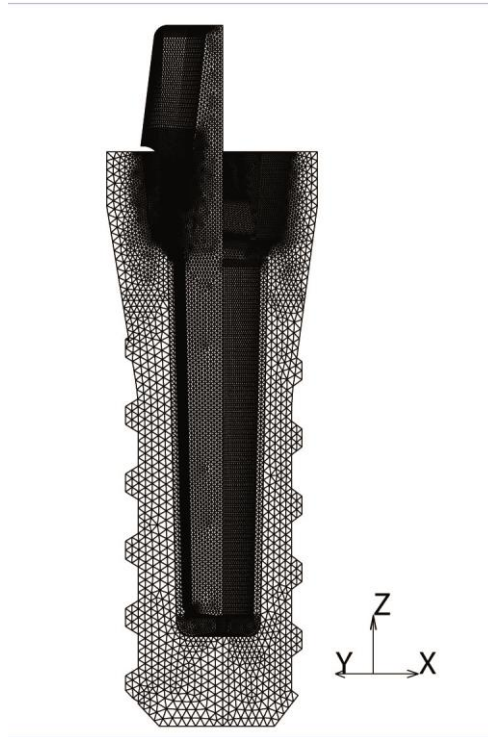


Fig. 16: FE mesh of CAD model 1 (IM-R11_standard, 120° model) for the screw-in simulation (278825 elements, 446918 nodes).

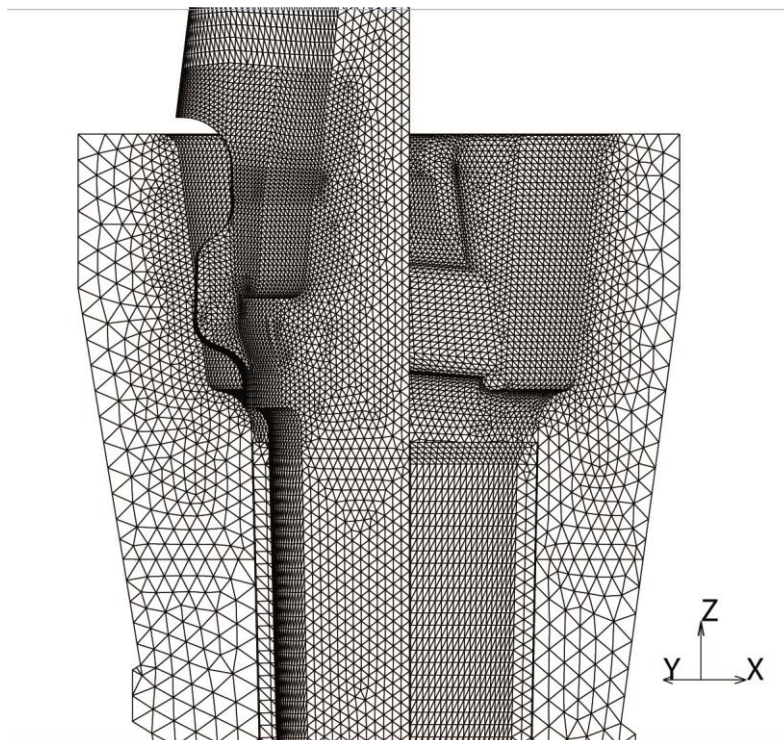


Fig. 17: Detail of Fig. 16.

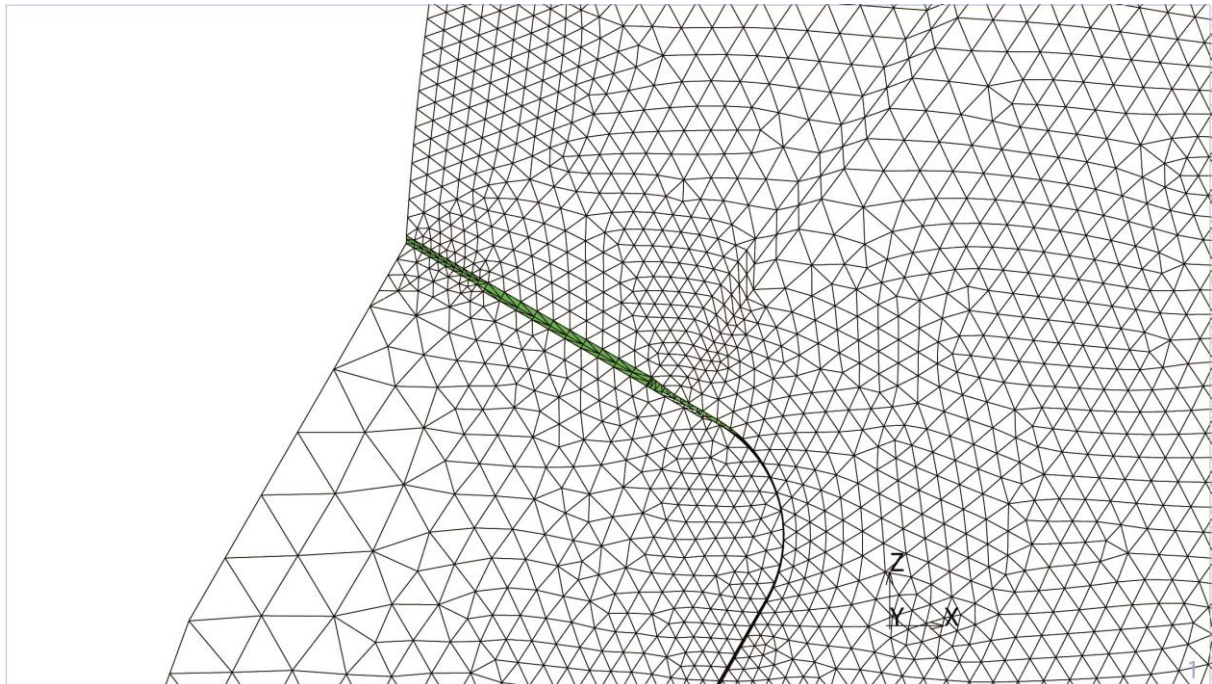


Fig. 18: FE mesh of CAD model 1b (IM-R11_standard with gap; +30°) with 1183058 elements, 1867110 nodes.

sk

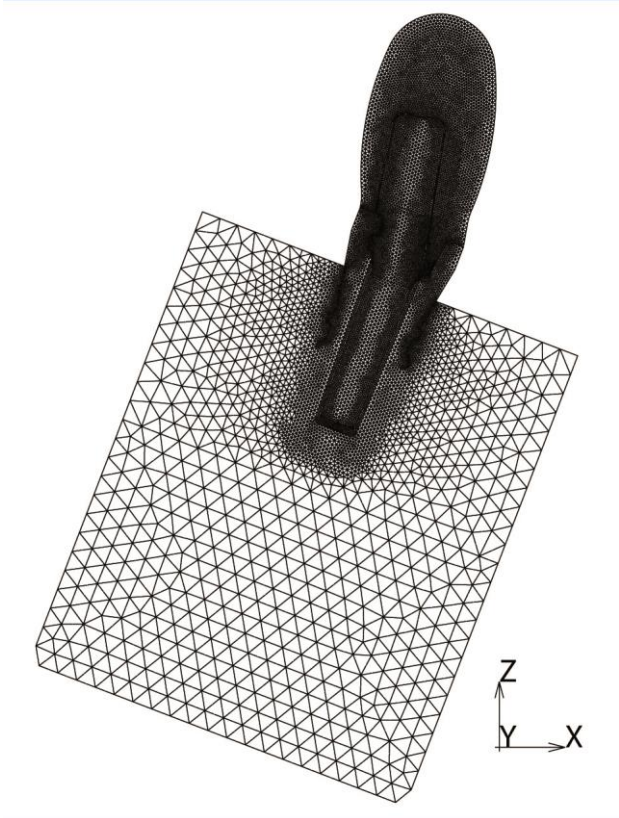


Fig. 19: FE mesh of CAD model 2 (IM-R11_individuell) with 1086542 elements, 1732531 nodes).

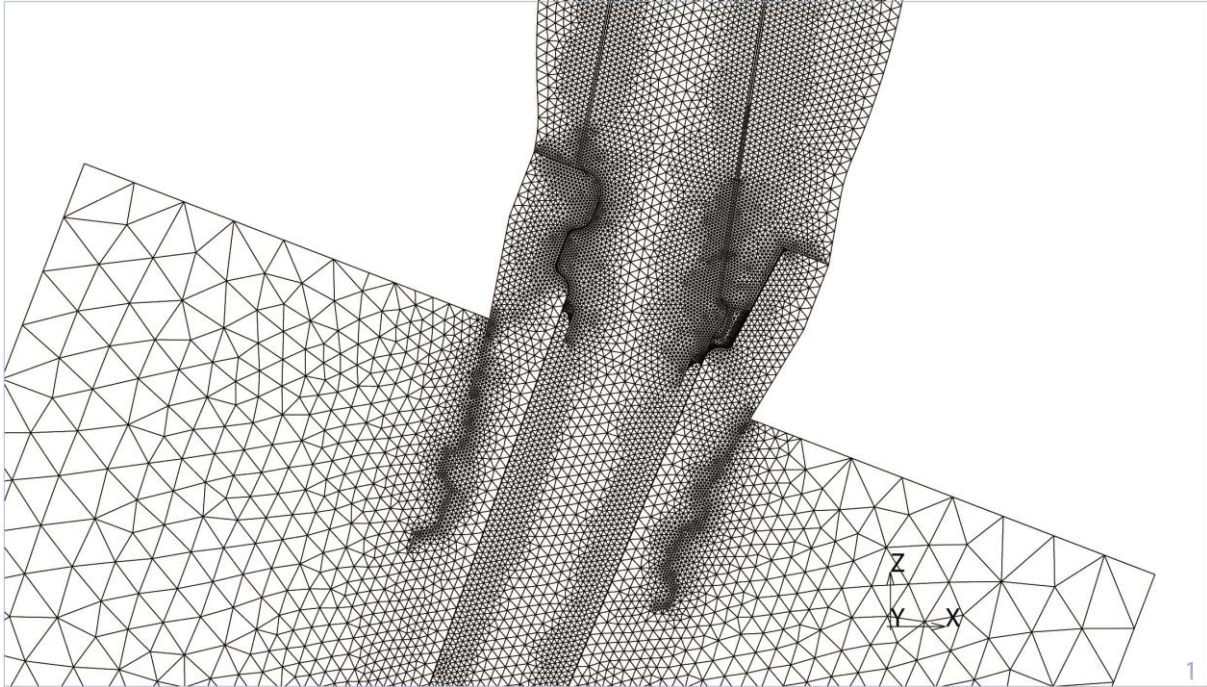


Fig. 20: Detail of Fig. 19.

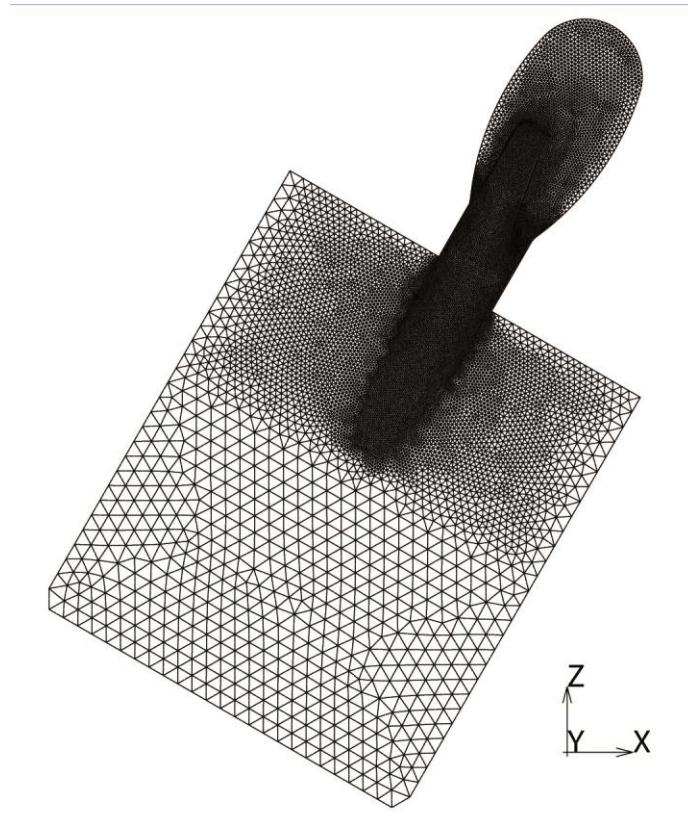


Fig. 21: FE mesh of CAD model 3 (IE-SST-L11; +30°) with 851137 elements, 1341923 nodes.

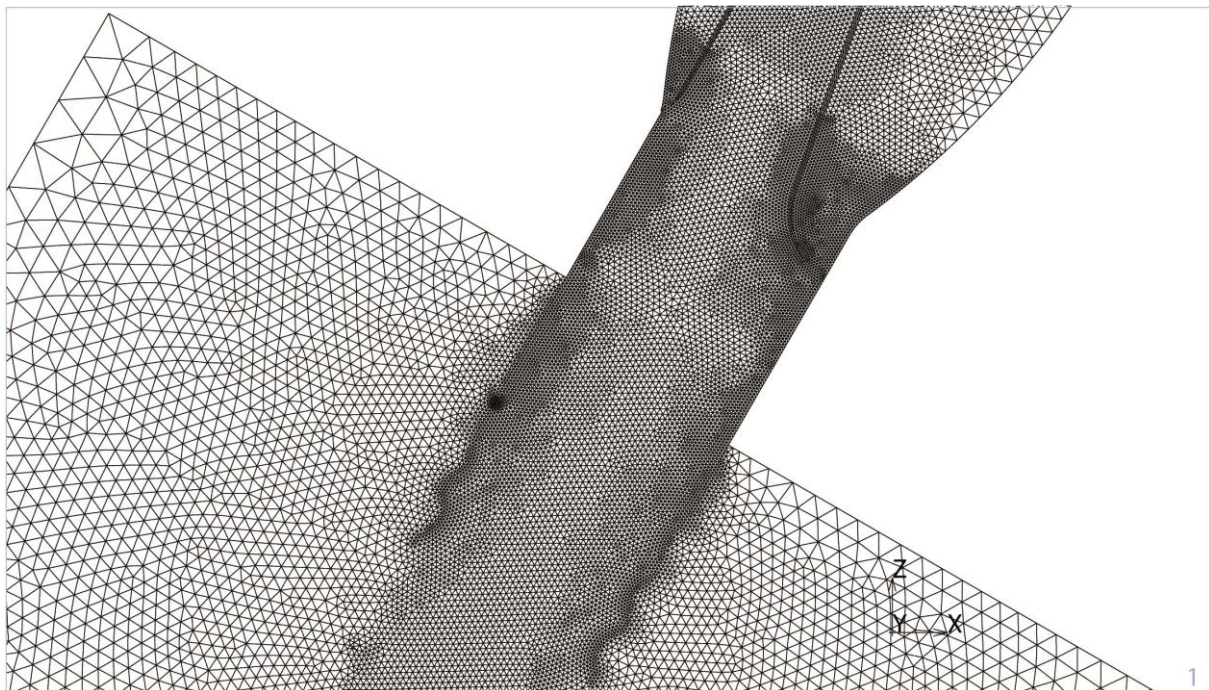


Fig. 22: Detail of Fig. 21.

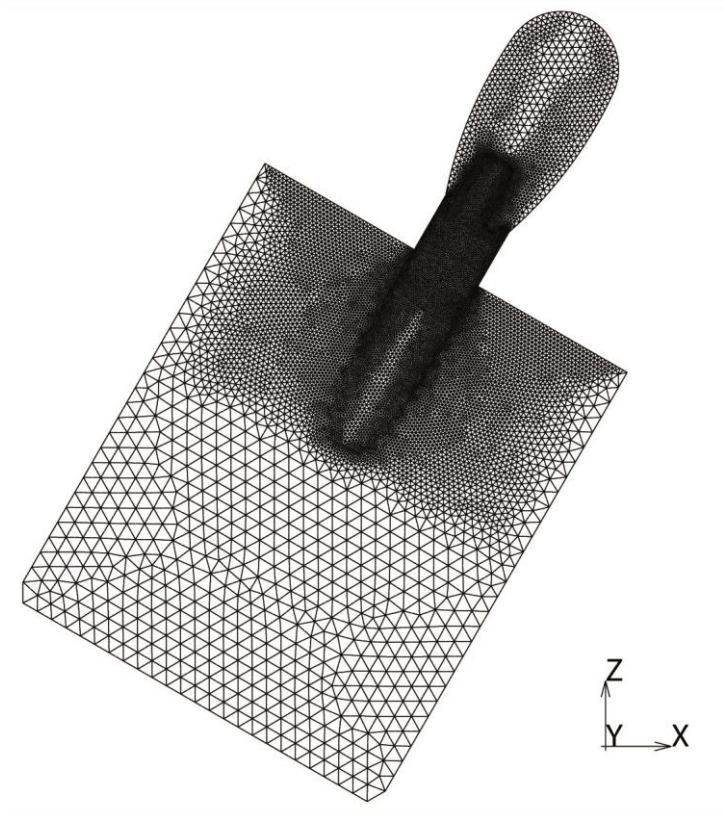


Fig. 23: FE mesh of CAD model 4 (IE-SBE-L11) with 963131 elements, 1184326 nodes.

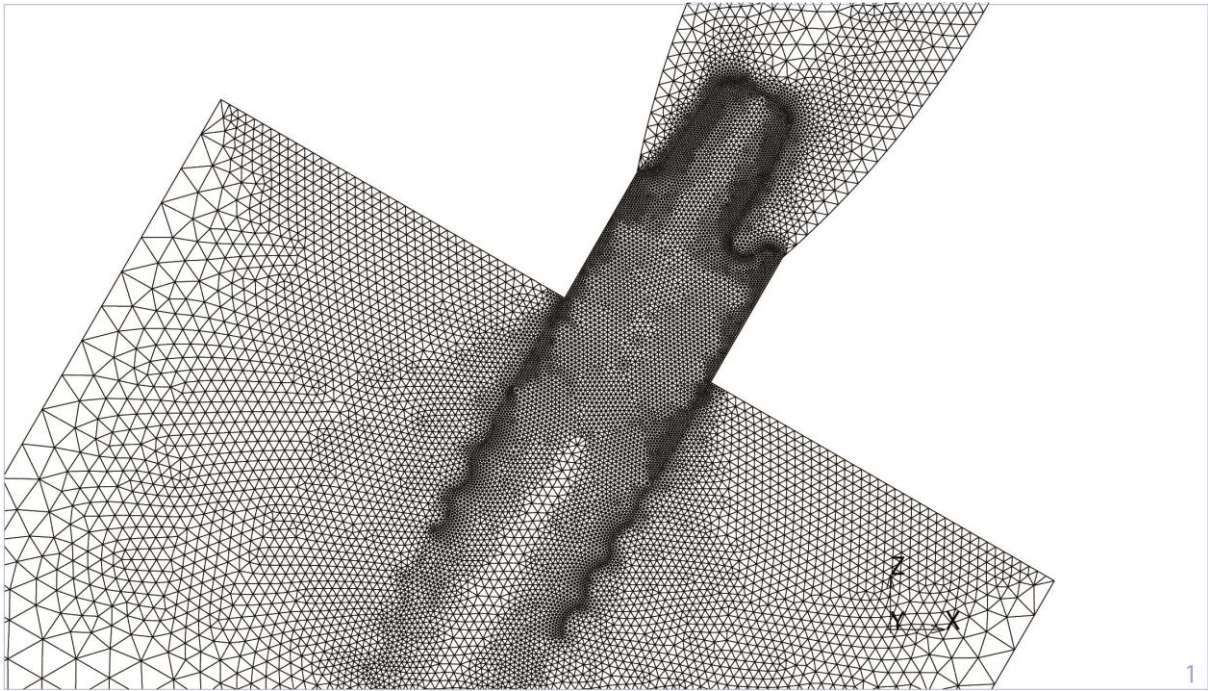


Fig. 24: Detail of Fig. 23.

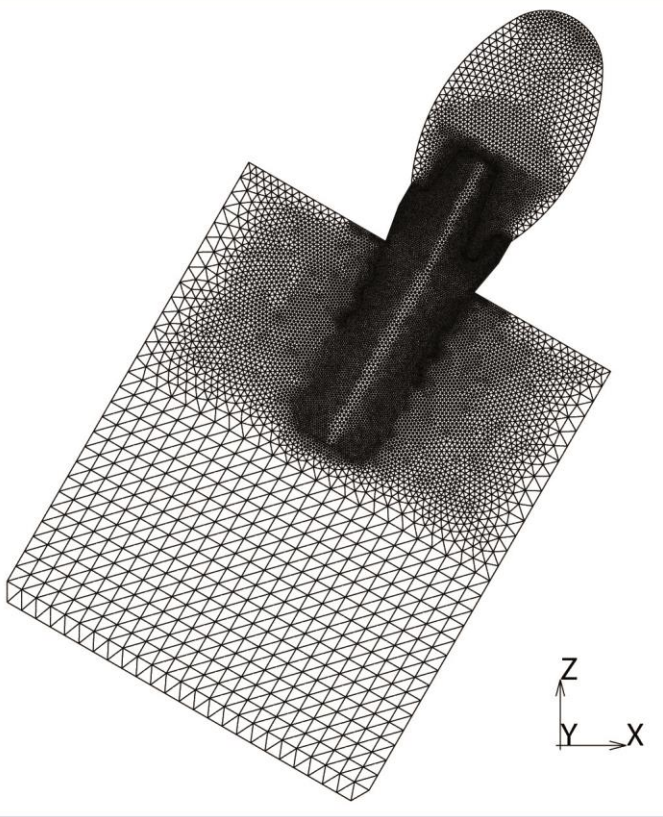


Fig. 25: FE mesh of CAD model 5 (IE-R-L11) with 977739 elements, 1581390 nodes.

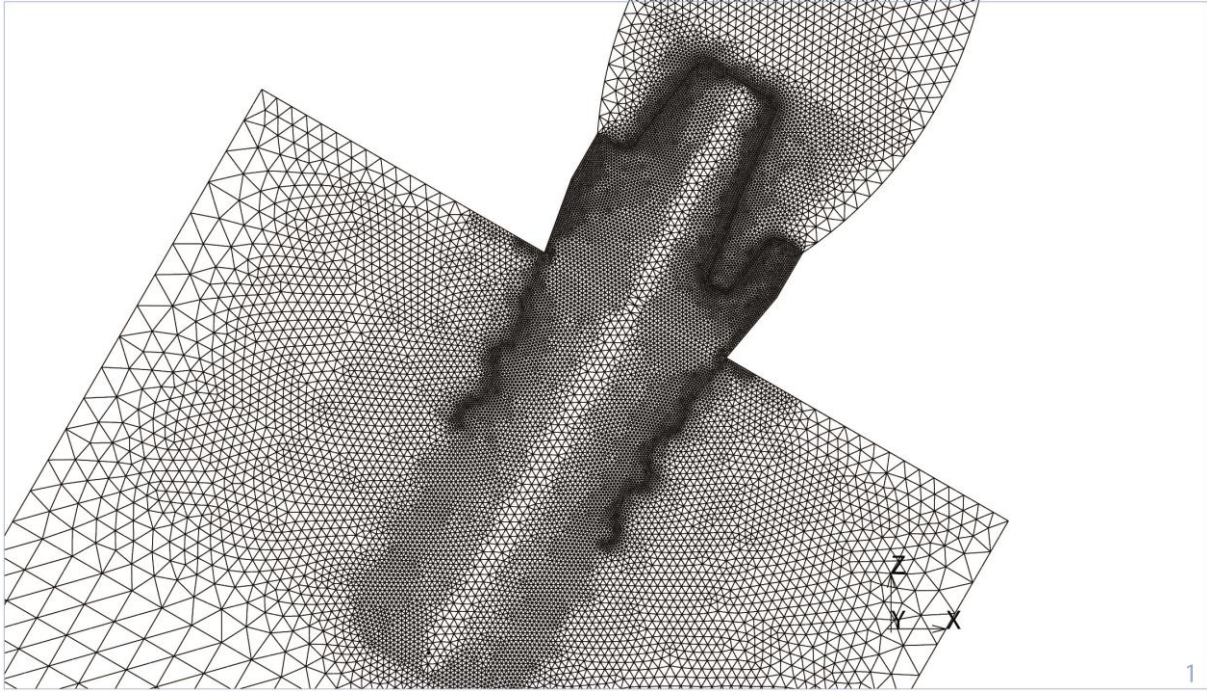


Fig. 26: Detail of Fig. 25.



Fig. 27: FE mesh of CAD model_6 (IM-2x_R11_indi-Abut_Bridge_11G) with 1145033 elements, 1716764 nodes (half model).

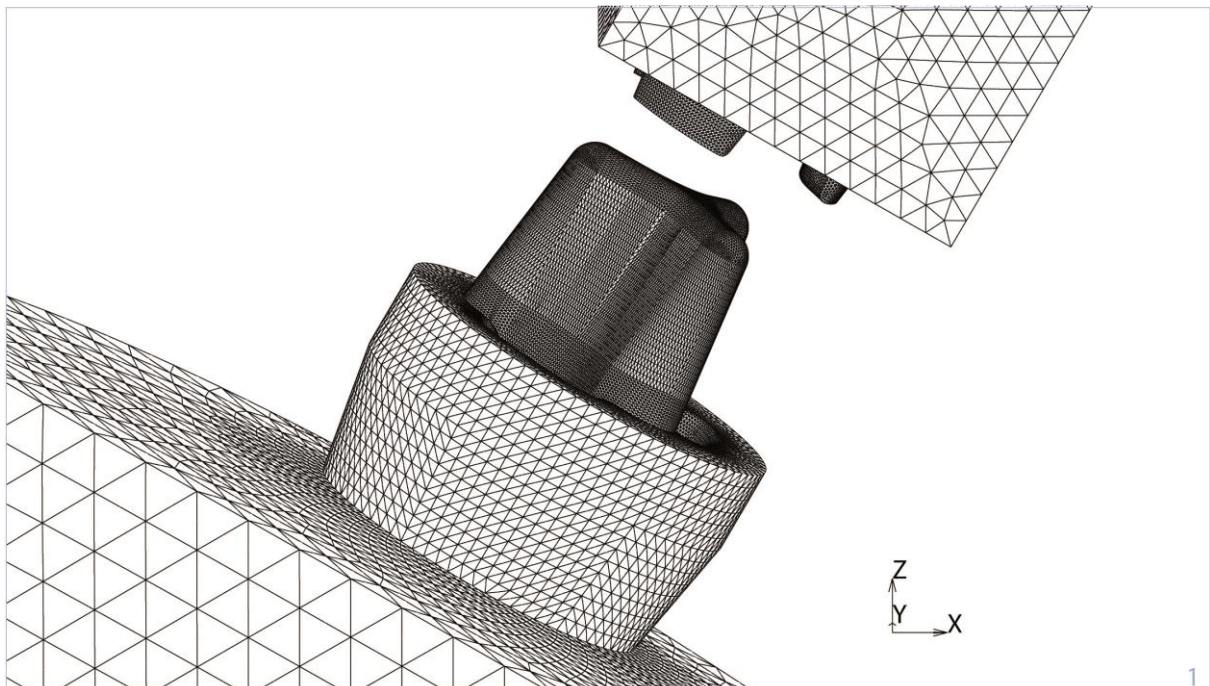


Fig. 28: Detail of Fig. 27. The bridge is lifted in this view.

FEA model 1 (+30°): Vertical load 200 N

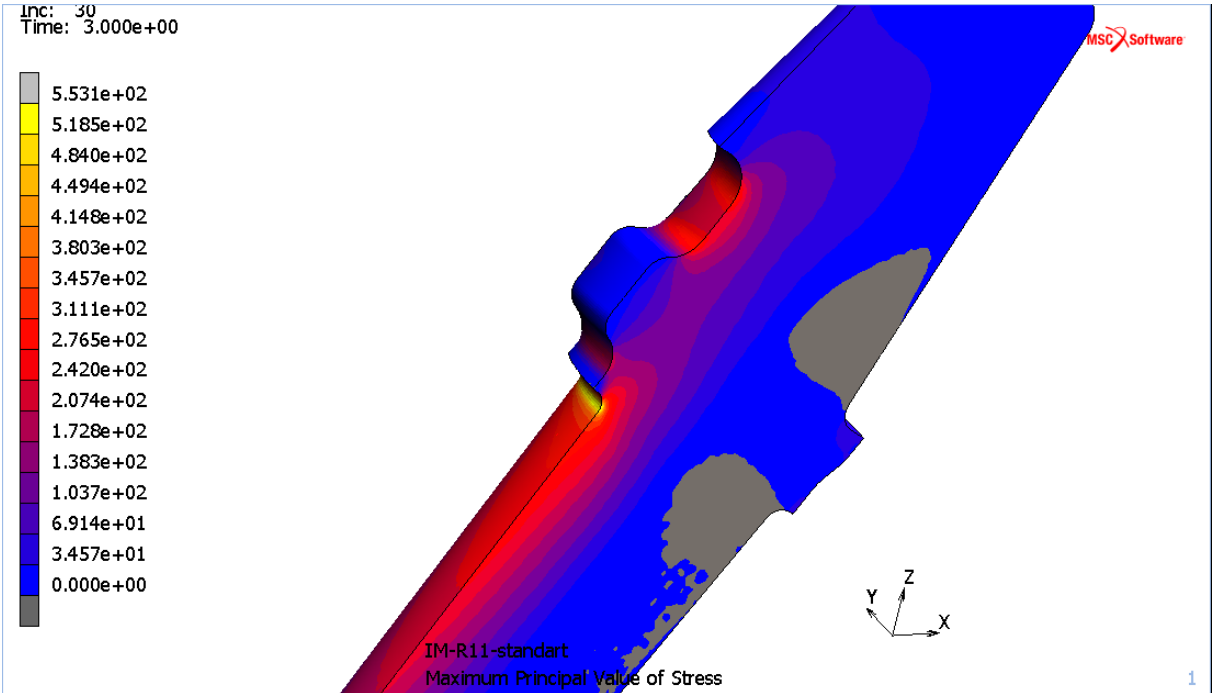


Fig. 34: FEA model 1 (+30°), load 200 N, abutment: Maximum principal stresses [MPa].

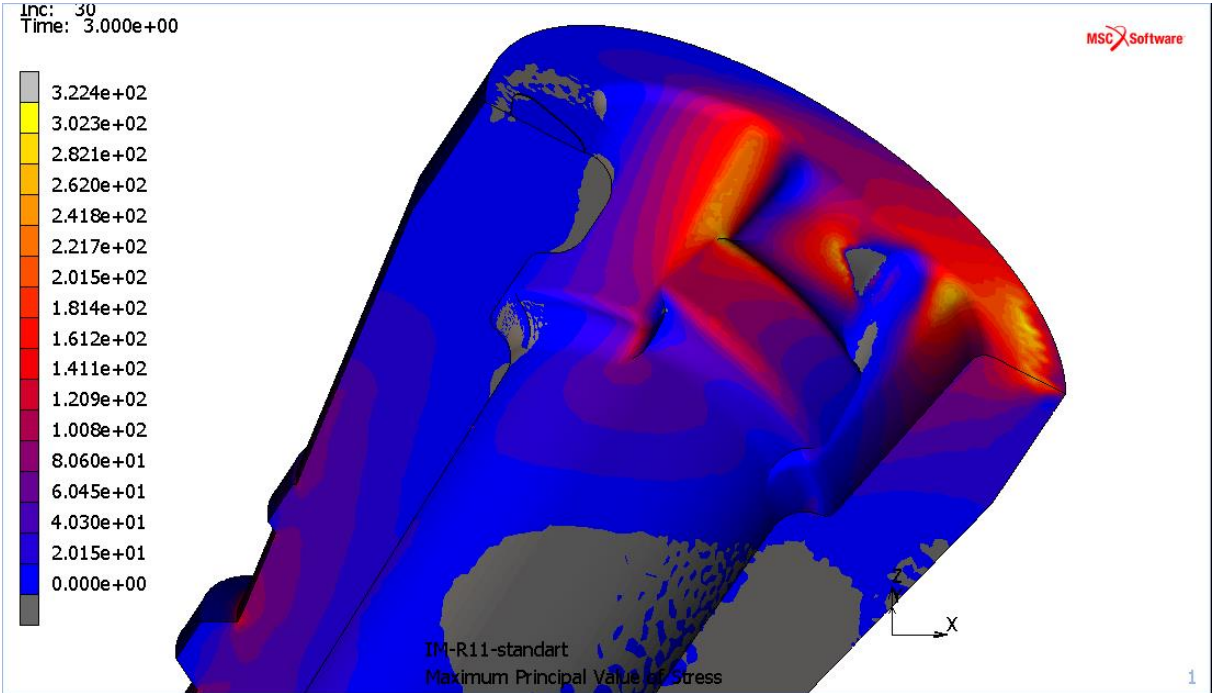


Fig. 35: FEA model 1 (+30°), load 200 N, implant body: Maximum principal stresses [MPa].

FEA model 1b (CAD model IM-R11_standard with gap)

Tab. 3 shows the maximum principal stresses in the implant components under the vertical load of 200 N under +30°.

Tab. 4: Maximum tensile principal stress values. Vertical load 200 N under +30°.

| FEA Model 1b (CAD model IM-R11_standard with gap) | Max. principal stress |
|--|-----------------------|
| Loading member | 63 MPa |
| Abutment | 90 MPa |
| Implant body | 252 MPa |

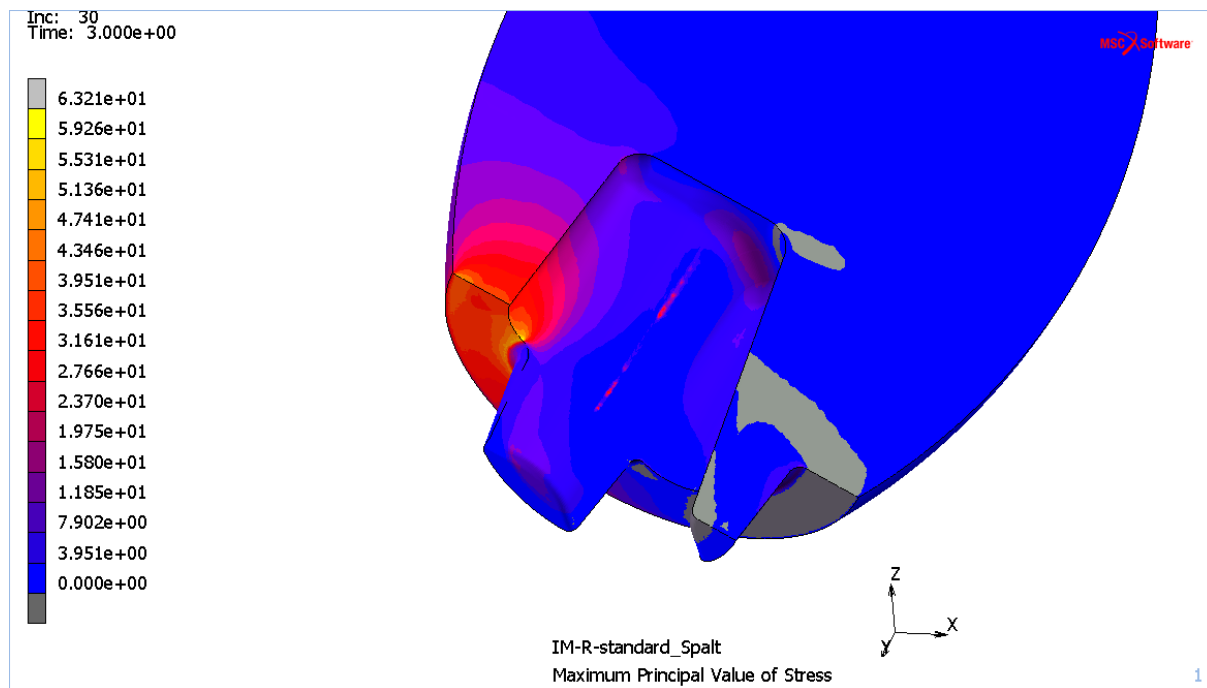


Fig. 36: FEA model 1b (+30°), load 200 N, loading member: Maximum principal stresses [MPa].

FEA model 2 (+21°): Vertical load 200 N

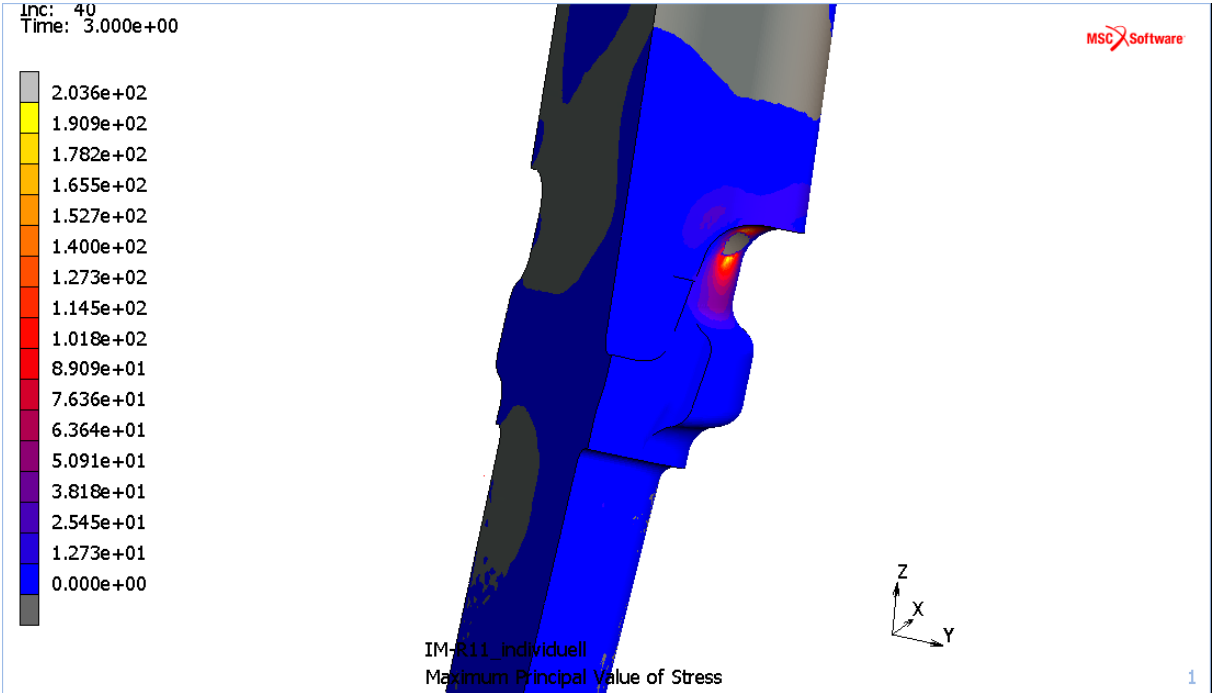


Fig. 40: FEA model 2 (+21°), load 200 N, abutment: Maximum principal stresses [MPa].

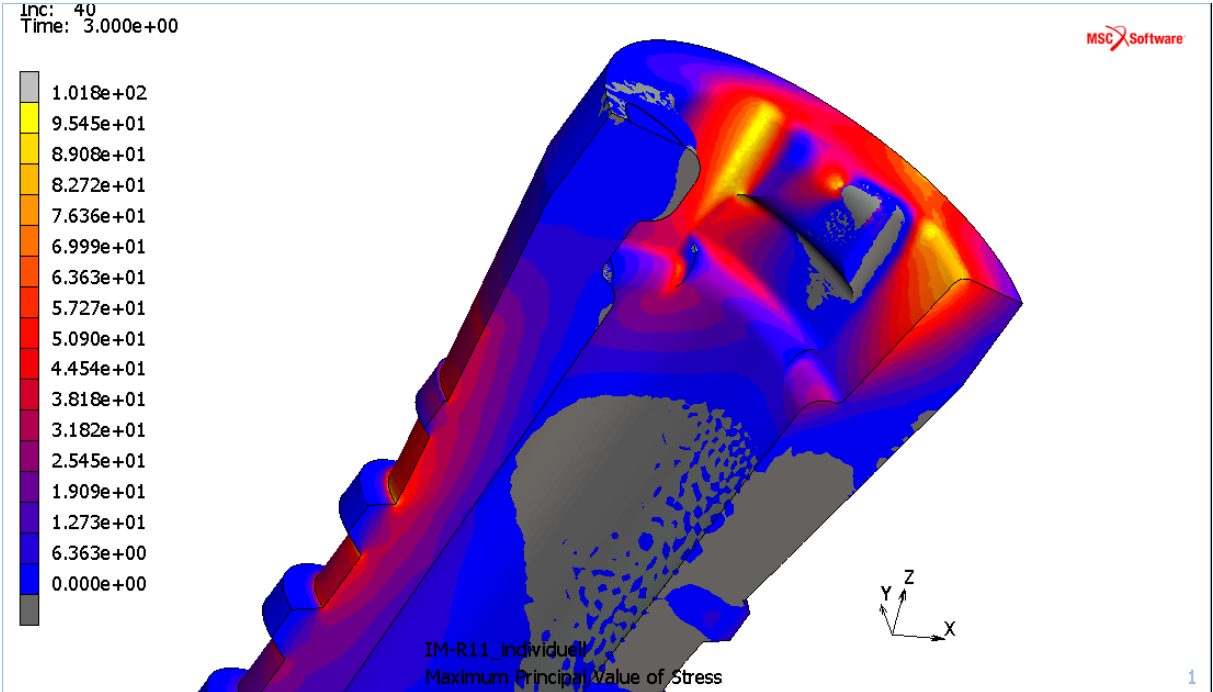


Fig. 41: FEA model 2 (+21°), load 200 N, implant body: Maximum principal stresses [MPa].

5.3 FEA model 3 (CAD model IE-SST-L11)

Tab. 6 shows the maximum principal stresses in the implant components at the vertical load of 200 N under +30°.

Tab. 6: Maximum tensile principal stress values. Vertical load 200 N under +30°.

| FEA Model 3 (CAD model IE-SST-L11) | Max. principal stress |
|---|----------------------------------|
| Loading member | 295 MPa |
| Implant | 337 MPa |

FEA model 3 (+30°): Vertical load 200 N

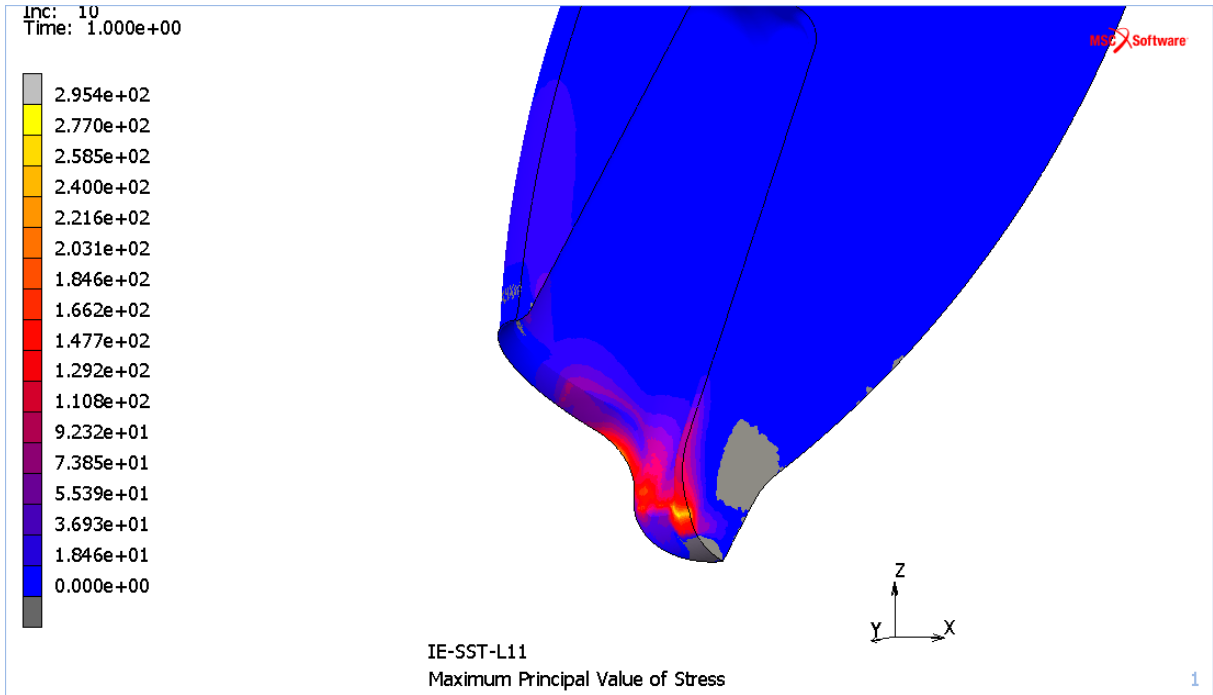


Fig. 42: FEA model 3 (+30°), load 200 N, loading member: Maximum principal stresses [MPa].

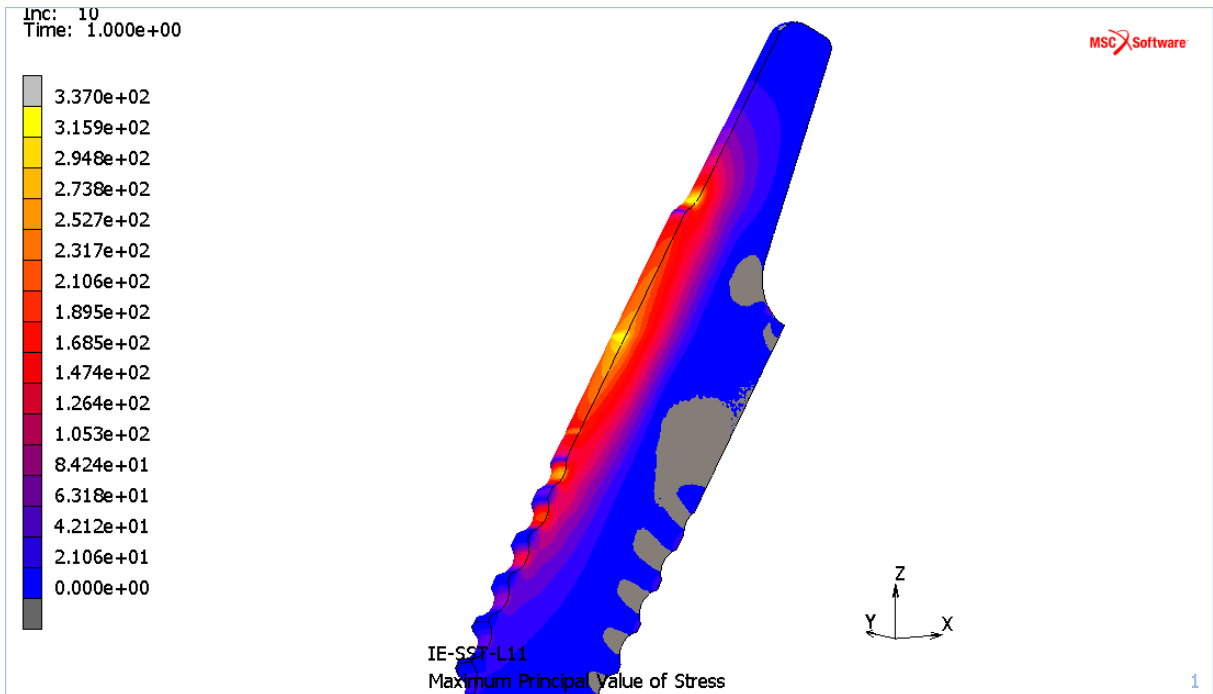


Fig. 43: FEA model 3 (+30°), load 200 N, implant: Maximum principal stresses [MPa].

5.4 FEA model 4 (CAD model IE-SBE-L11)

Tab. 7 shows the maximum principal stresses in the implant components at the vertical load of 200 N under +30°.

Tab. 7: Maximum tensile principal stress values.

| FEA Model 4 (CAD model IE-SBE-L11) | Max. principal stress |
|---|----------------------------------|
| Loading member | 137 MPa |
| Implant | 336 MPa |

FEA model 4 (+30°): Vertical load 200 N

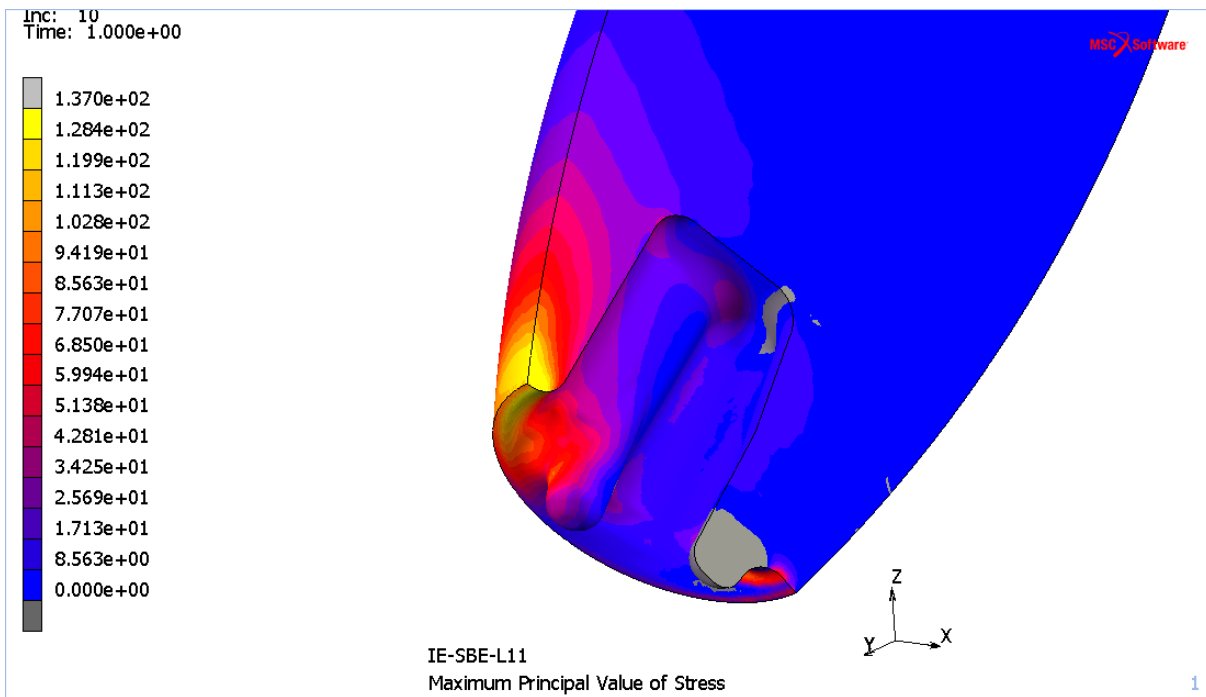


Fig. 44: FEA model 4 (+30°), load 200 N, loading member: Maximum principal stresses [MPa].

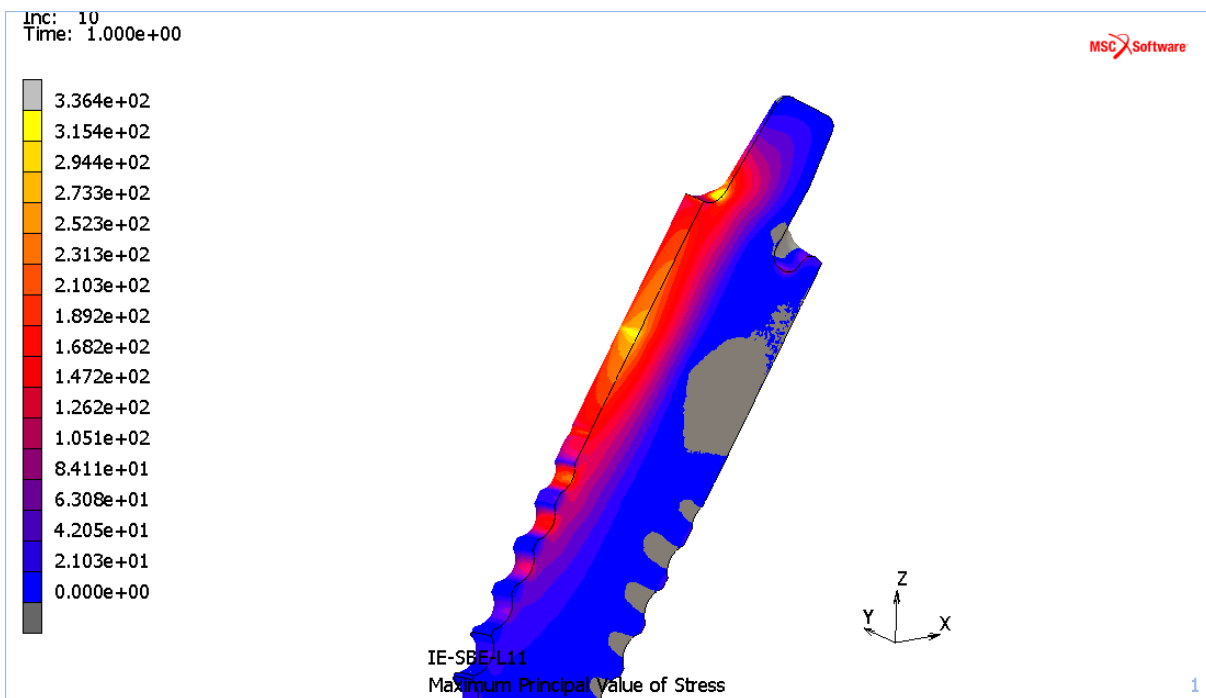


Fig. 45: FEA model 4 (+30°), load 200 N, implant: Maximum principal stresses [MPa].

5.5 FEA model 5 (CAD model IE-SST-L11)

Tab. 8 shows the maximum principal stresses in the implant components at the vertical load of 200 N under -30°.

Tab. 8: Maximum tensile principal stress values.

| FEA Model 5 (CAD model IE-SST-L11) | Max. principal stress |
|---|----------------------------------|
| Loading member | 265 MPa |
| Implant | 518 MPa |

5.6 FEA model 6 (CAD model IE-R-L11)

Tab. 9 shows the maximum principal stresses in the implant components at the vertical load of 200 N under +30°.

Tab. 9: Maximum tensile principal stress values.

| FEA Model 6 (CAD model IE-R-L11) | Max. principal stress |
|---|----------------------------------|
| Loading member | 242 MPa |
| Implant | 241 MPa |

5.7 FEA model 7 (CAD model IM-R11_standard)

Tab. 10 shows the maximum principal stresses in the implant components at the vertical load of 200 N under -30° .

Tab. 10: Maximum tensile principal stress values. Vertical load 200 N under -30° .

| FEA Model 7 (CAD model IM-R11_standard) | Max. principal stress |
|--|-----------------------|
| Loading member | 250 MPa |
| Abutment | 496 MPa |
| Implant body | 319 MPa |

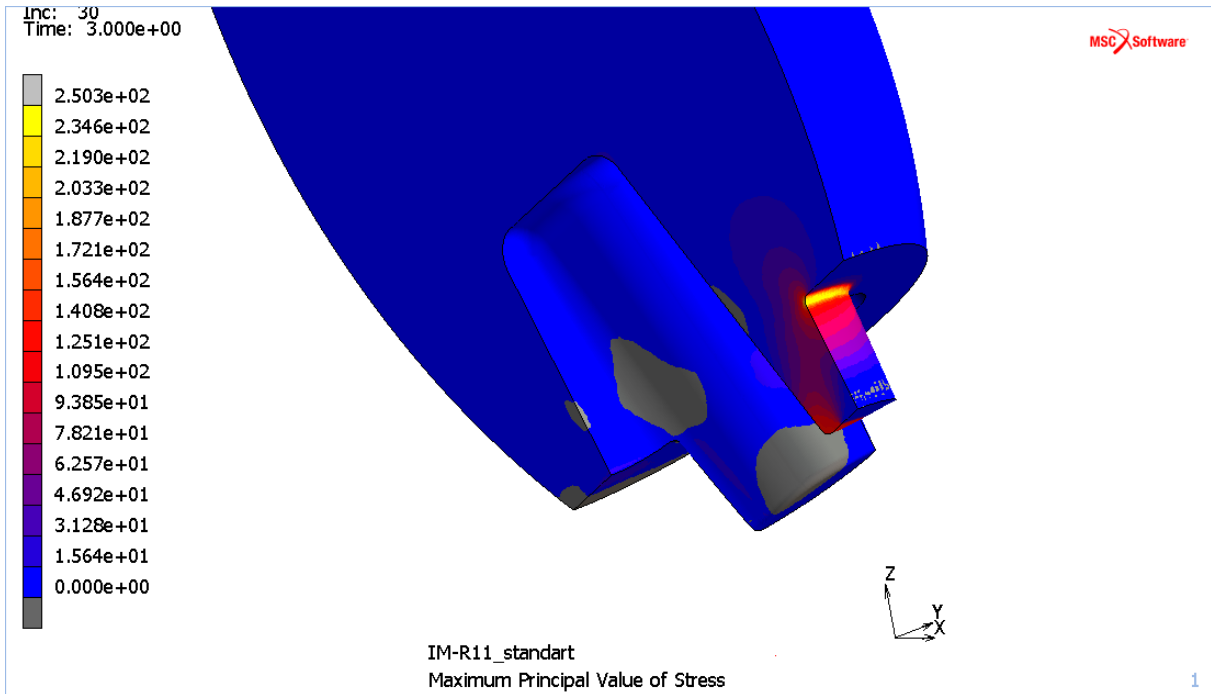


Fig. 50: FEA model 7 (-30°), load 200 N, loading member: Maximum principal stresses [MPa].

5.8 FEA model 8 (CAD model IM-R11_standard)

Tab. 11 shows the maximum principal stresses in the implant components after the screw-in of the abutment into the implant body.

Tab. 11: Maximum tensile principal stress values.

| FEA Model 8 (CAD model IM-R11_standard) | Max. principal stress |
|--|----------------------------------|
| Abutment | 25 MPa |
| Implant body | 31 MPa |

FEA model 8, screw-in of the abutment

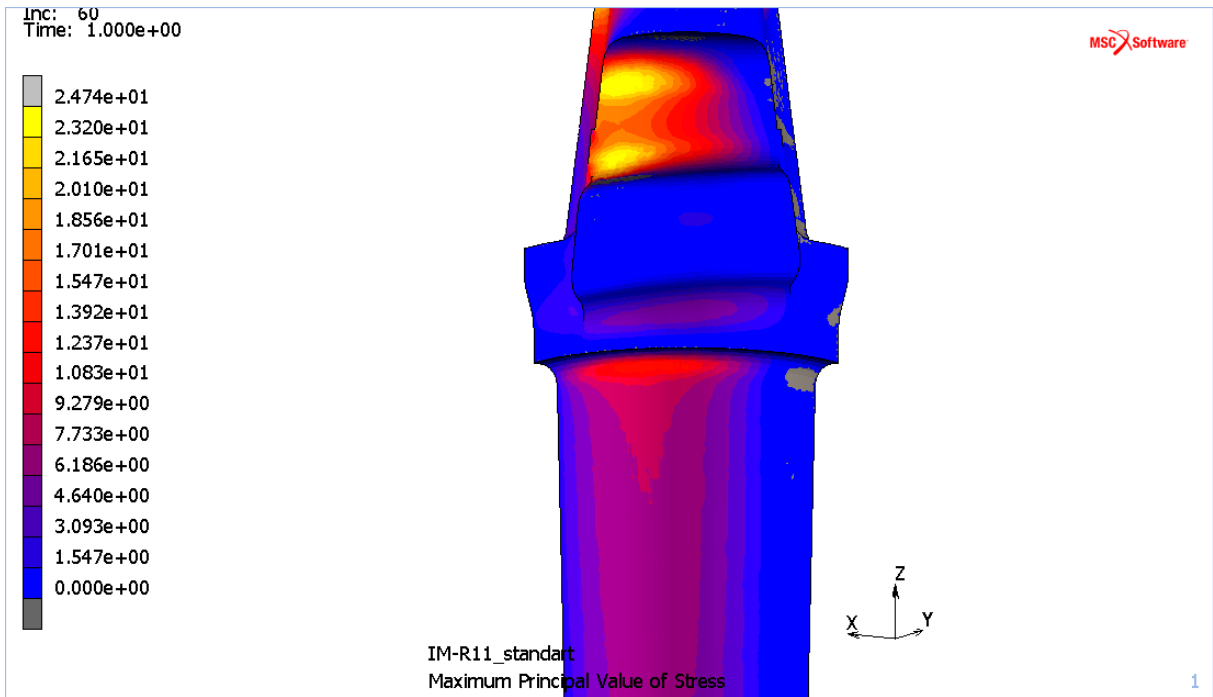


Fig. 53: FEA model 8, abutment: Maximum principal stresses [MPa].

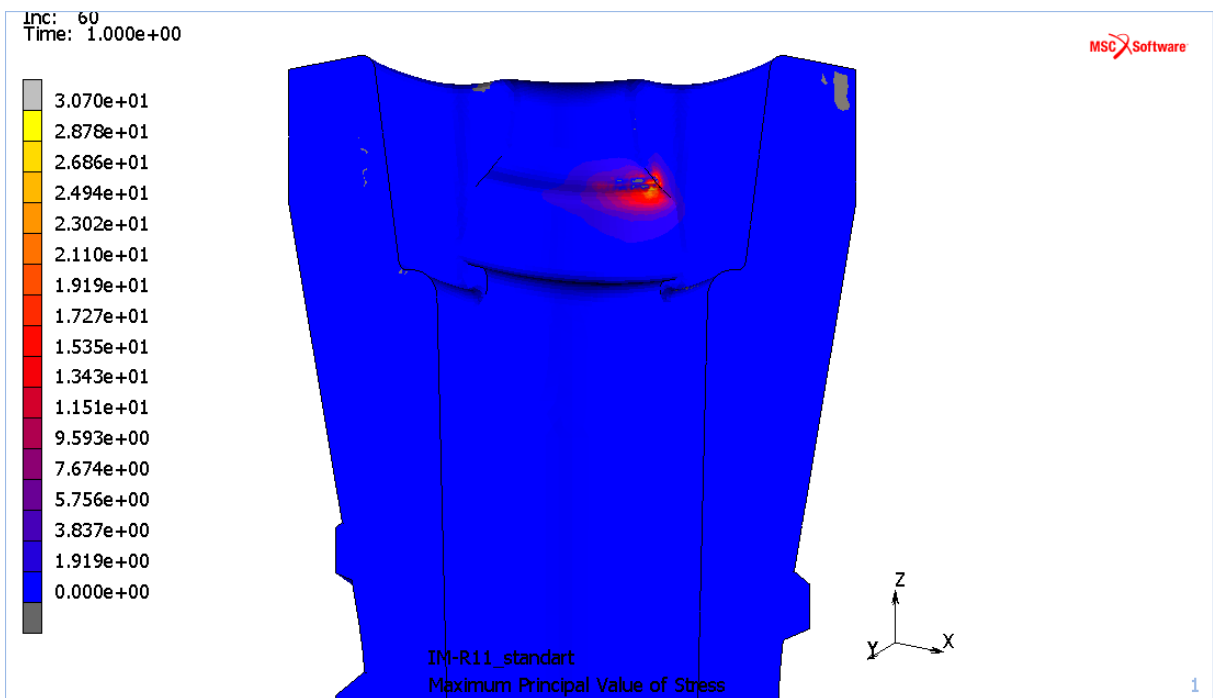


Fig. 54: FEA model 8, implant body: Maximum principal stresses [MPa].

FEA model 9 (+30°): Vertical load 200 N

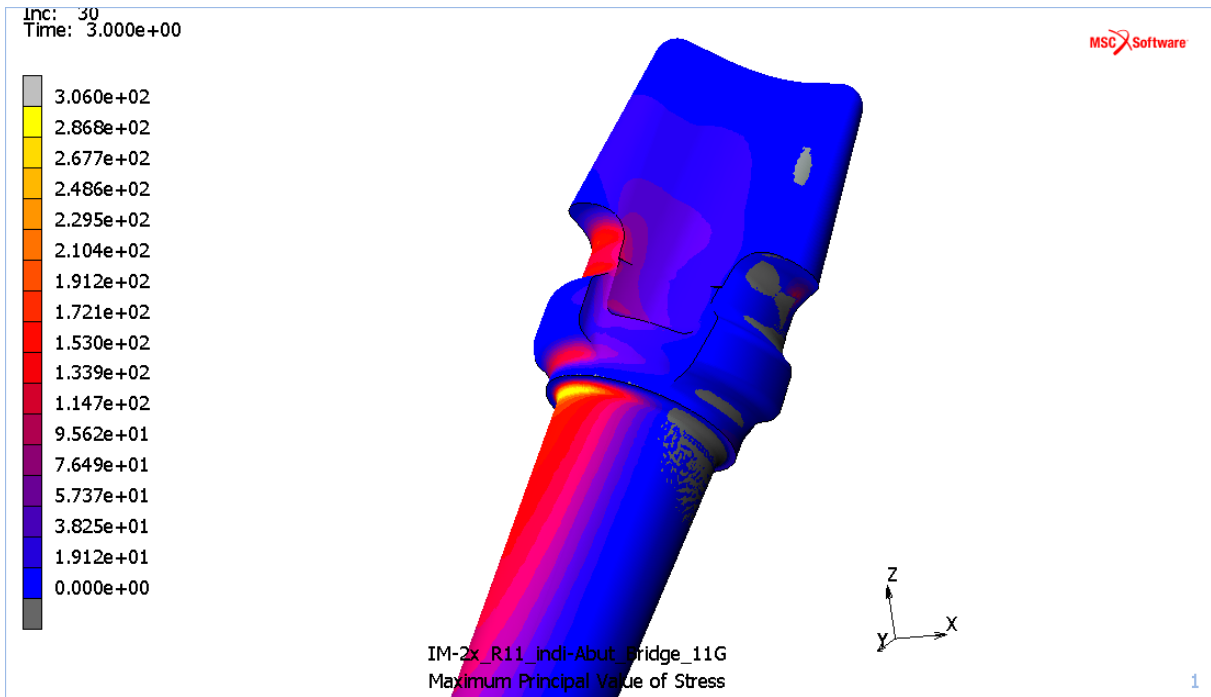


Fig. 56: FEA model 9 (+30°), load 200 N, abutment: Maximum principal stresses [MPa].

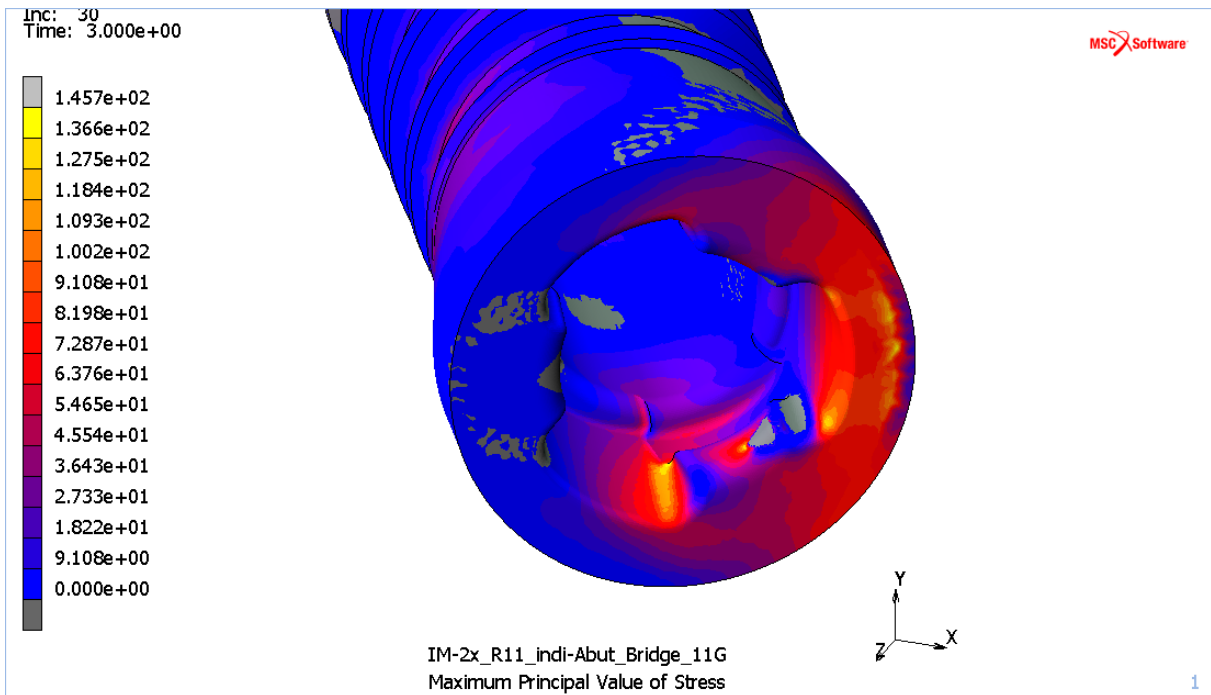


Fig. 57: FEA model 9 (+30°), load 200 N, implant body: Maximum principal stresses [MPa].

FEA model 10 (+30°): Vertical load 200 N

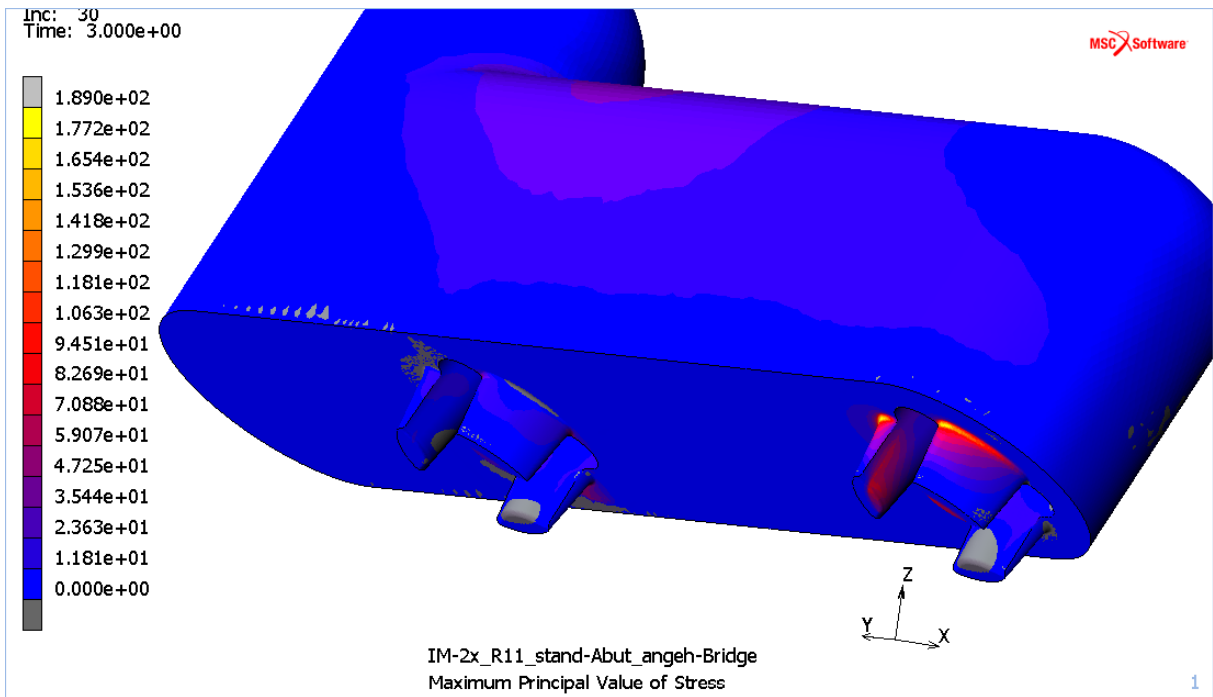


Fig. 59: FEA model 10 (+30°), load 200 N, loading member: Maximum principal stresses [MPa].

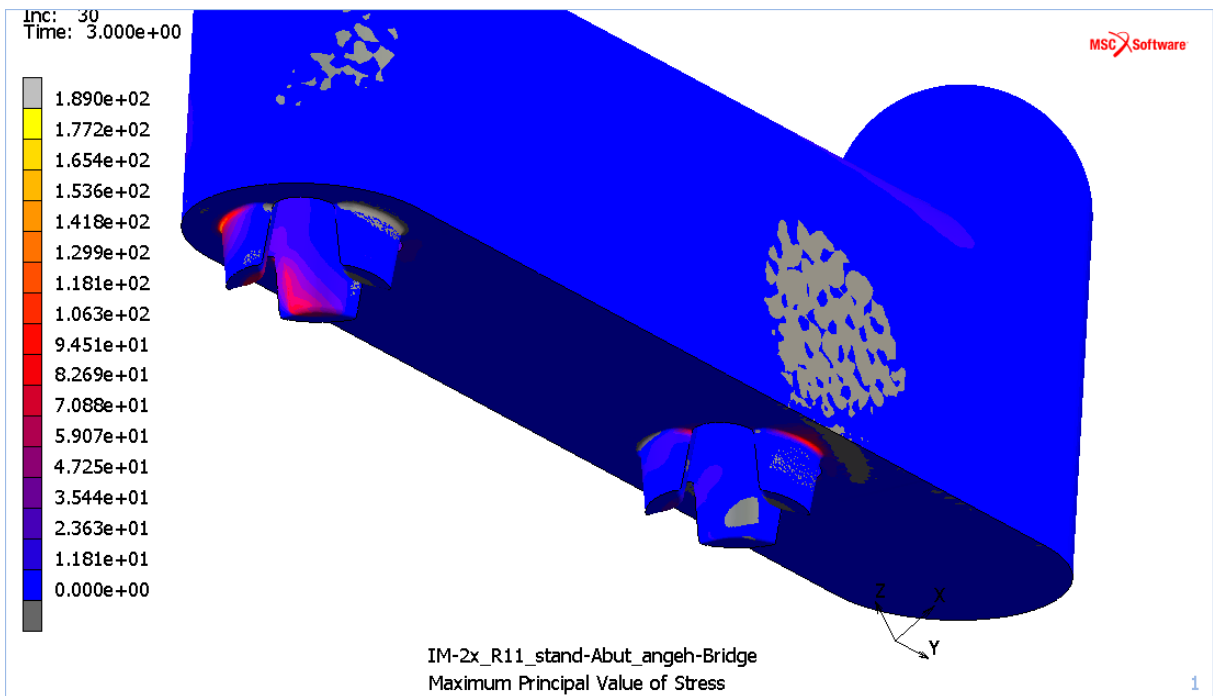


Fig. 60: FEA model 10 (+30°), load 200 N, loading member: Maximum principal stresses [MPa].

FEA model 10 (+30°): Vertical load 200 N

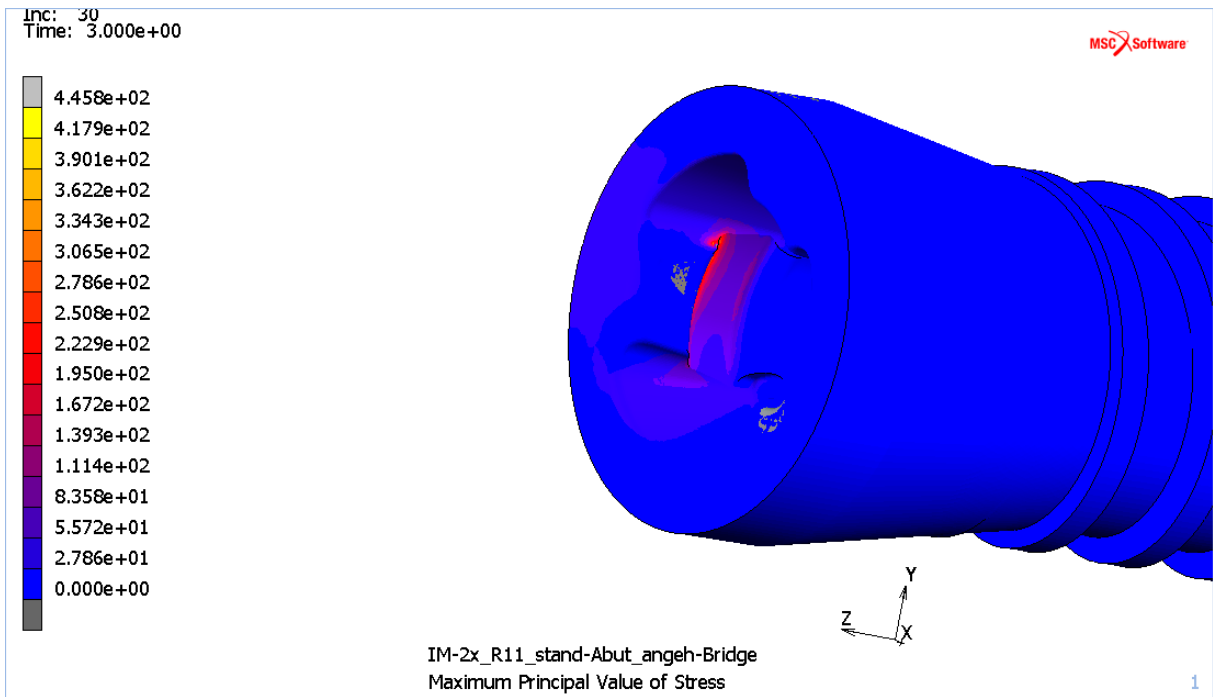


Fig. 65: FEA model 10 (+30°), load 200 N, implant body 1: Maximum principal stresses [MPa].

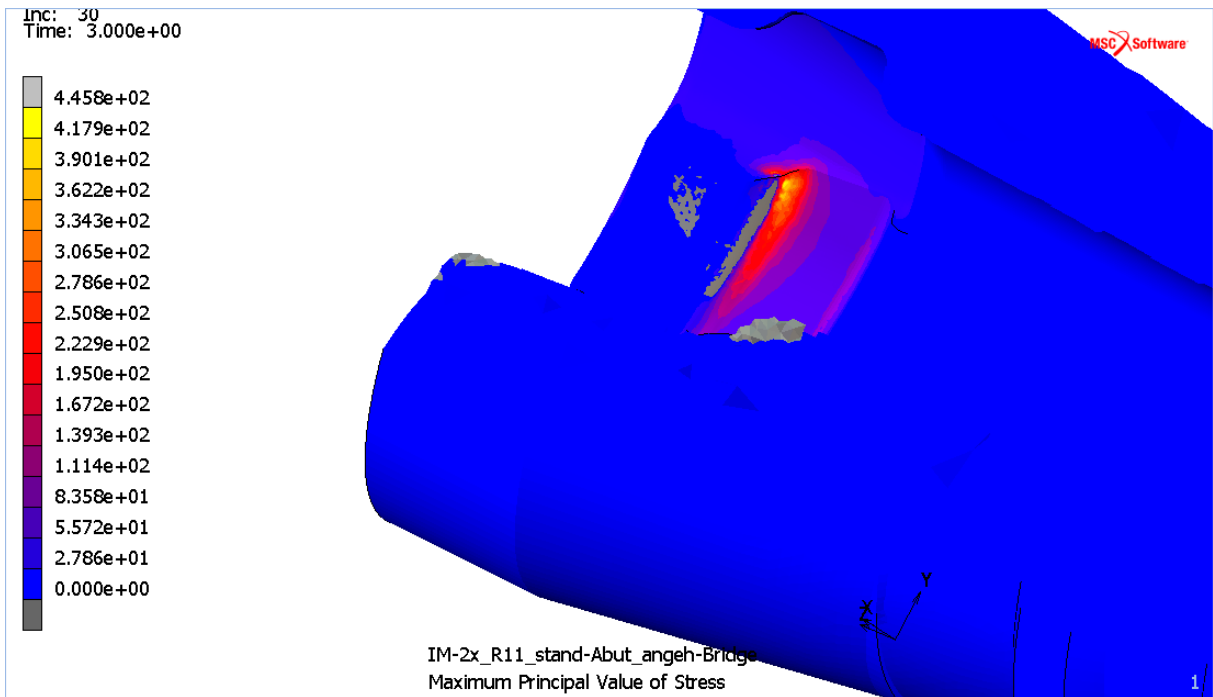


Fig. 66: FEA model 10 (+30°), load 200 N, implant body 1: Maximum principal stresses [MPa].

FEA model 10 (+30°): Vertical load 200 N

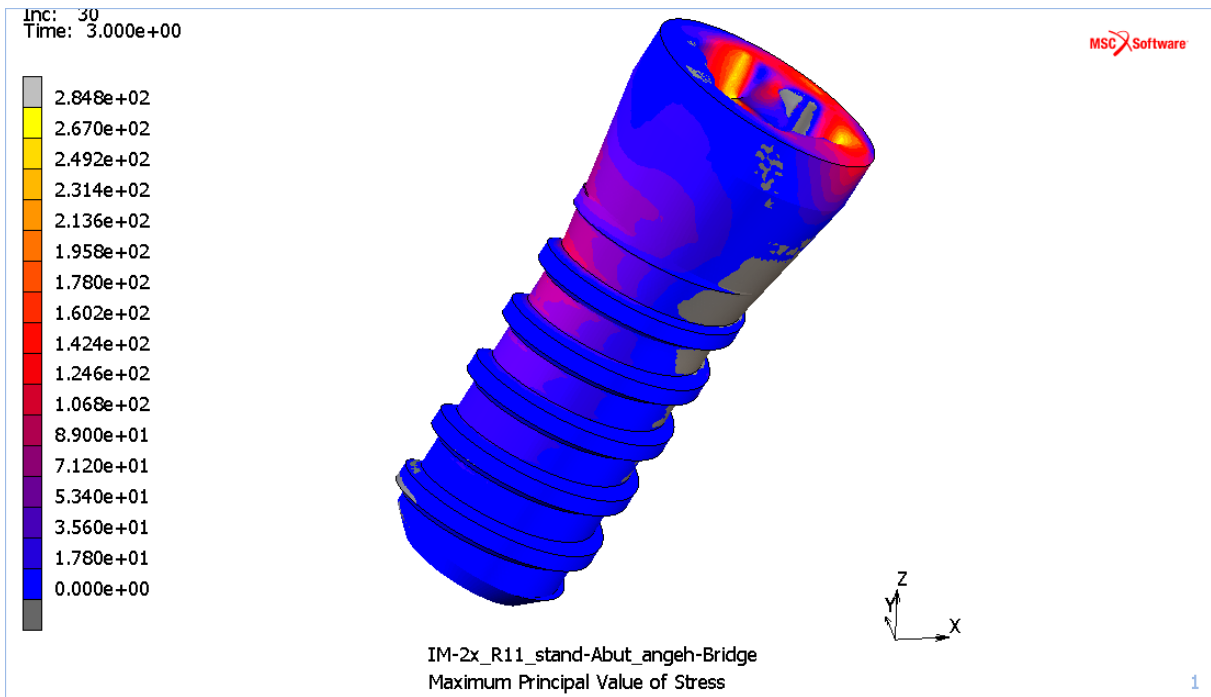


Fig. 67: FEA model 10 (+30°), load 200 N, implant body 2: Maximum principal stresses [MPa].

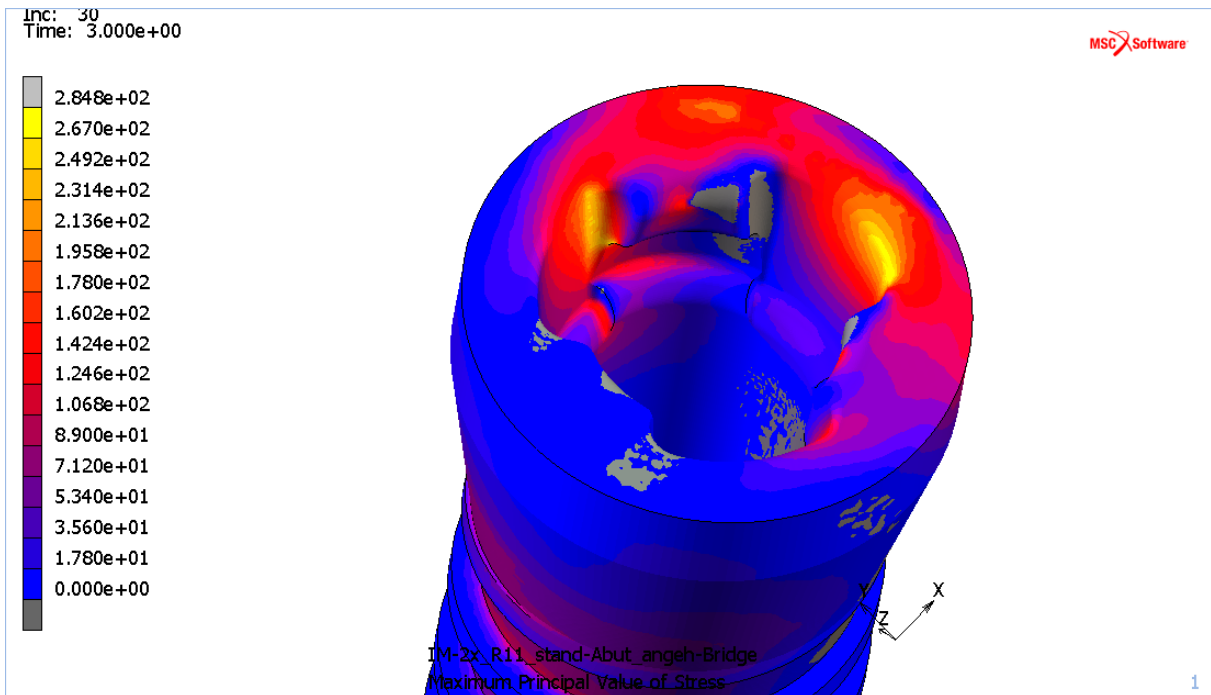


Fig. 68: FEA model 10 (+30°), load 200 N, implant body 2: Maximum principal stresses [MPa].

5.11 FEA model 11 (CAD model ZSystems Z5c)

Tab. 14 shows the maximum principal stresses in the implant components at the vertical load of 200 N under +30°.

Tab. 14: Maximum tensile principal stress values.

| FEA Model 11 (CAD model ZSystems Z5c) | Max. principal stress |
|--|----------------------------------|
| Loading member | 163 MPa |
| Abutment | 350 MPa |
| Implant body | 832 MPa |

FEA model 11 (+30°): Vertical load 200 N

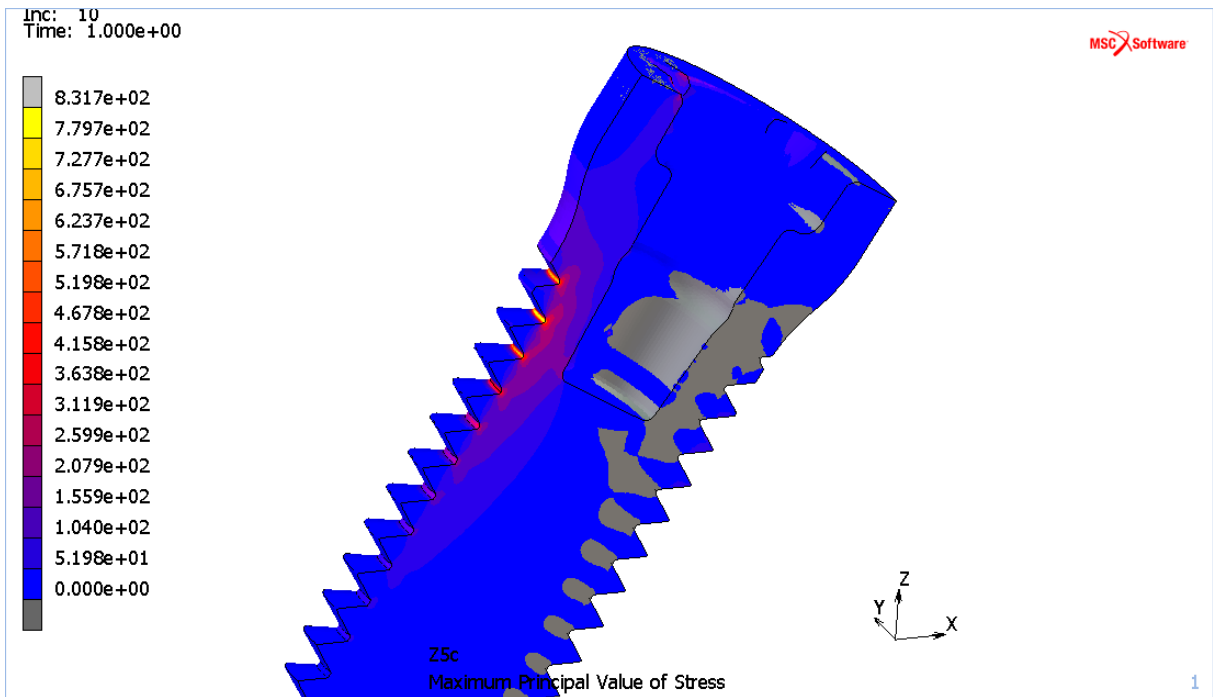


Fig. 73: FEA model 11 (+30°), load 200 N, implant body: Maximum principal stresses [MPa].

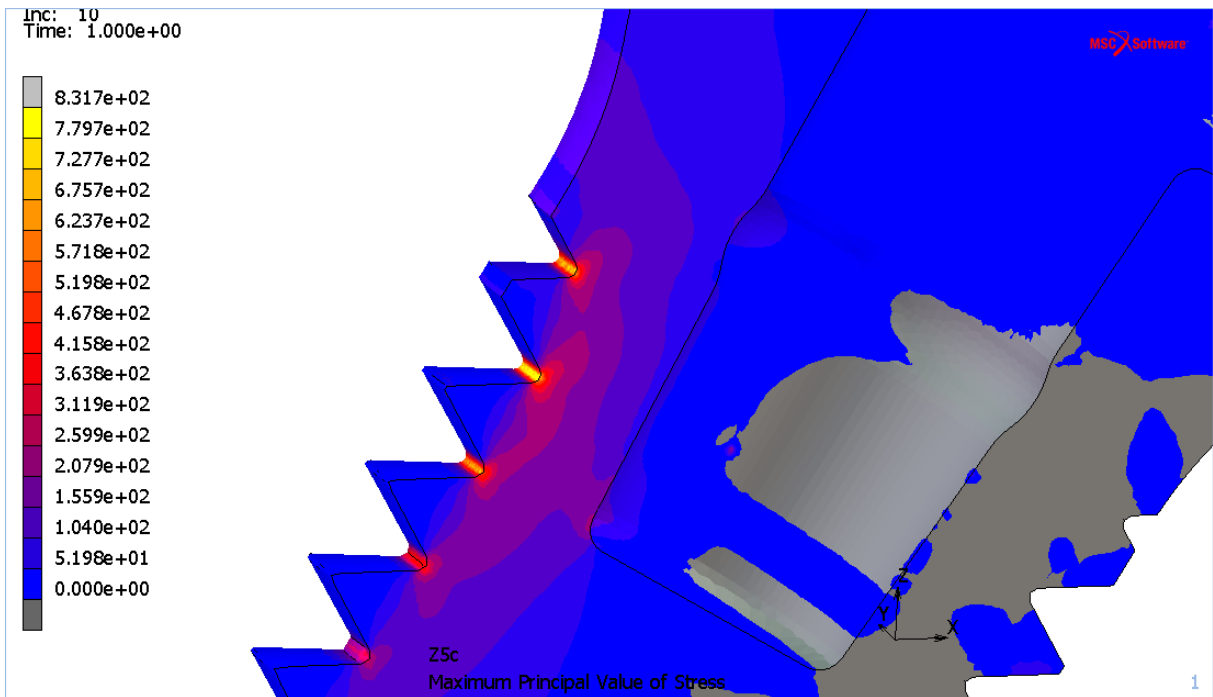


Fig. 74: FEA model 11 (+30°), load 200 N, implant body: Maximum principal stresses [MPa].

6 Conclusion

The Finite Element Analyses performed within this report were used to compare different setups and systems among each other. All analyses have been run under an axial load of 200 N.

All models mentioned below refer to the overview shown in Tab. 1. All stress values mentioned are tensile principal stresses.

The stress values in FEA model 1 (max. value 553 MPa in the abutment) were higher compared to FEA model 2 (max. value 291 MPa in the loading member).

Therefore FEA model 1 with the non-angulated abutment can be considered as the worst case compared to model 2 with the angulated abutment.

In FEA model 1b (IM-R11_standard with gap) no gap was seen under loading as a glued cement layer has been positioned between loading member and the implant body shoulder.

The stress values are clearly lower in all components compared to FEA model 1 (IM-R11_standard) under the load of 200 N.

The comparison between the multi-part implants (FEA model 1 and FEA model 2) and the single-part implant systems (FEA model 3 to 6) show higher stress values in FEA model 1 and 2.

Loading the single-part implant system IE-SST-L11 under -30° (FEA model 5) the maximum stress in the implant increased to 518 MPa compared to the 30° loading (FEA model 3) with a maximum stress value of 337 MPa.

The multi-part implant IM-R11_standard (FEA model 1) loaded under $+30^\circ$ showed higher stresses (max. value 553 MPa) compared to the same implant system under -30° (FEA model 7, max. value 496 MPa).

The simulation of the screw-in of the abutment into sleeve/implant body of the multi-part implant IM-R11_standard (FEA model 8) showed a maximum stress value of 31 MPa in the implant body.

Both bridge models were also loaded with 200 N and showed a lower maximum stress value (306 MPa in the abutment) in bridge model IM-2x_R11_indi-Abut_Bridge_11G (FEA model 9) compared to the maximum stress value of 446 MPa in the bridge model IM-2x_R11_stand-Abut_angeh-Bridge (FEA model 10).

Comparing all Zirkonus models (FEA model 1 to FEA model 10) with the ZSystems model Z5c (FEA model 11) showed that in the Z5c model the overall maximum stresses were found in the implant body (maximum stress value 832 MPa).

Due to the lack of data regarding the cements used, no conclusions can be drawn regarding a possible failure or detachment of the cement within the simulated models.